Marine and Petroleum Geology 121 (2020) 104639

Contents lists available at ScienceDirect

Marine and Petroleum Geology

journal homepage: www.elsevier.com/locate/marpetgeo

Research paper

Regional controls in the distribution and morphometry of deep-water gravitational deposits along a convergent tectonic margin. Southern Caribbean of Colombia

J. Naranjo-Vesga [a,b,*], A. Ortiz-Karpf [a], L. Wood [c], Z. Jobe [c], J.F. Paniagua-Arroyave [b,d], L. Shumaker [c], D. Mateus-Tarazona [a,b], P. Galindo [a]

[a] Ecopetrol S.A, Instituto Colombiano del Petróleo, Piedecuesta, Colombia
[b] Grupo de Ciencias del Mar, Departamento de Ciencias de la Tierra, Universidad EAFIT, Medellín, Colombia
[c] Department of Geology and Geological Engineering, Colorado School of Mines, Golden, CO, 80401, USA
[d] Department of Earth, Ocean and Atmospheric Science, Florida State University, Tallahassee, FL, USA

ARTICLE INFO

Keywords:
Southern Caribbean of Colombia
Deep-water fold and thrust belt
Deep-water gravitational deposits
Channel-levee systems
Submarine canyons
Sediment supply
Slope profile
Shelf width

ABSTRACT

Deep-water fold and thrust belts often develop in convergent tectonic margins, creating irregular slope profiles that control the distribution of deep-water gravity deposits. However, in areas with high sediment supply, the erosion and sedimentation can minimize structural relief and smooth the slope. Using multibeam bathymetry with 3D seismic data, we analyze the distribution of deep-water gravity-driven deposits along the convergent margin of the southern Caribbean of Colombia, comparing areas with different continental sediment supply, slope profile, and shelf width. We identify three geomorphological zones: The Northern, Central and Southern Zones. The Northern Zone is characterized by a gentle slope topography, high sediment supply, and large (>100 km length) channel-levee systems traversing the slope and basin floor. In this zone, shelf-attached mass-transport deposits erode and smooth sea-floor topography. The Central Zone is characterized by low sediment supply and steep and irregular slope topography. Here, short-runout mass-transport deposits sourced from the crests and steep flanks of emergent anticlines are common. The irregular relief created by tectonic deformation forms barriers for sediment transport, leading to tortuous sediment-flow pathways. Submarine canyons incise the thrust-cored anticlines, transporting sediment through interconnected, adjacent piggyback sub-basins. Finally, the Southern Zone is characterized by steep slope and moderate sediment supply. Here, tectonic deformation has been smoothed by numerous shelf-attached mass-transport deposits. The erosional scours carved by mass flows merge downslope and evolve into submarine canyons that can deliver mass-transport deposits more than 80 km into the basin. We analyze the impact of slope profile, sediment input and shelf width on the distribution and morphology of deep-water deposits along the southern Colombian Caribbean margin, and present a predictive model for the depositional patterns more likely to develop in other continental margins affected by deep-water fold and thrust belts.

1. Introduction

Understanding the distribution and morphometry of deep-water sediment-gravity-flow deposits is of great importance to the energy industry due to their potential to contain hydrocarbons, and to the threat that they pose to submarine and coastal infrastructure (Clark and Cartwright, 2009; Mayall et al., 2010; Morley et al., 2011; Posamentier et al., 2000; Posamentier and Kolla, 2003; Shanmugam, 2016; Stow and Piper, 1984).

Along compressive margins, deep-water fold and thrust belts create highly irregular slope topographies that can strongly influence the distribution and morphometry of deep-water deposits (McAdoo et al., 2000; Smith, 2004). Steep anticlines transition rapidly to piggy-back sub-basins, both of which hinder sediment transport from the continental shelf to the basin floor. (Bourget et al., 2011; Cadena et al., 2015; Clark and Cartwright, 2009; Mayall et al., 2010; Morley et al., 2011; Morley and Leong, 2008; Romero-Otero, 2009; Vinnels et al., 2010). Sediment is supplied to the system not only by shelf-edge deltaic

* Corresponding author. Ecopetrol S.A. Instituto Colombiano del Petróleo, Kilómetro 7, vía Bucaramanga – Piedecuesta, Piedecuesta, Colombia.
E-mail address: julian.naranjo@ecopetrol.com.co (J. Naranjo-Vesga).

https://doi.org/10.1016/j.marpetgeo.2020.104639
Received 18 April 2020; Received in revised form 29 July 2020; Accepted 2 August 2020
Available online 6 August 2020

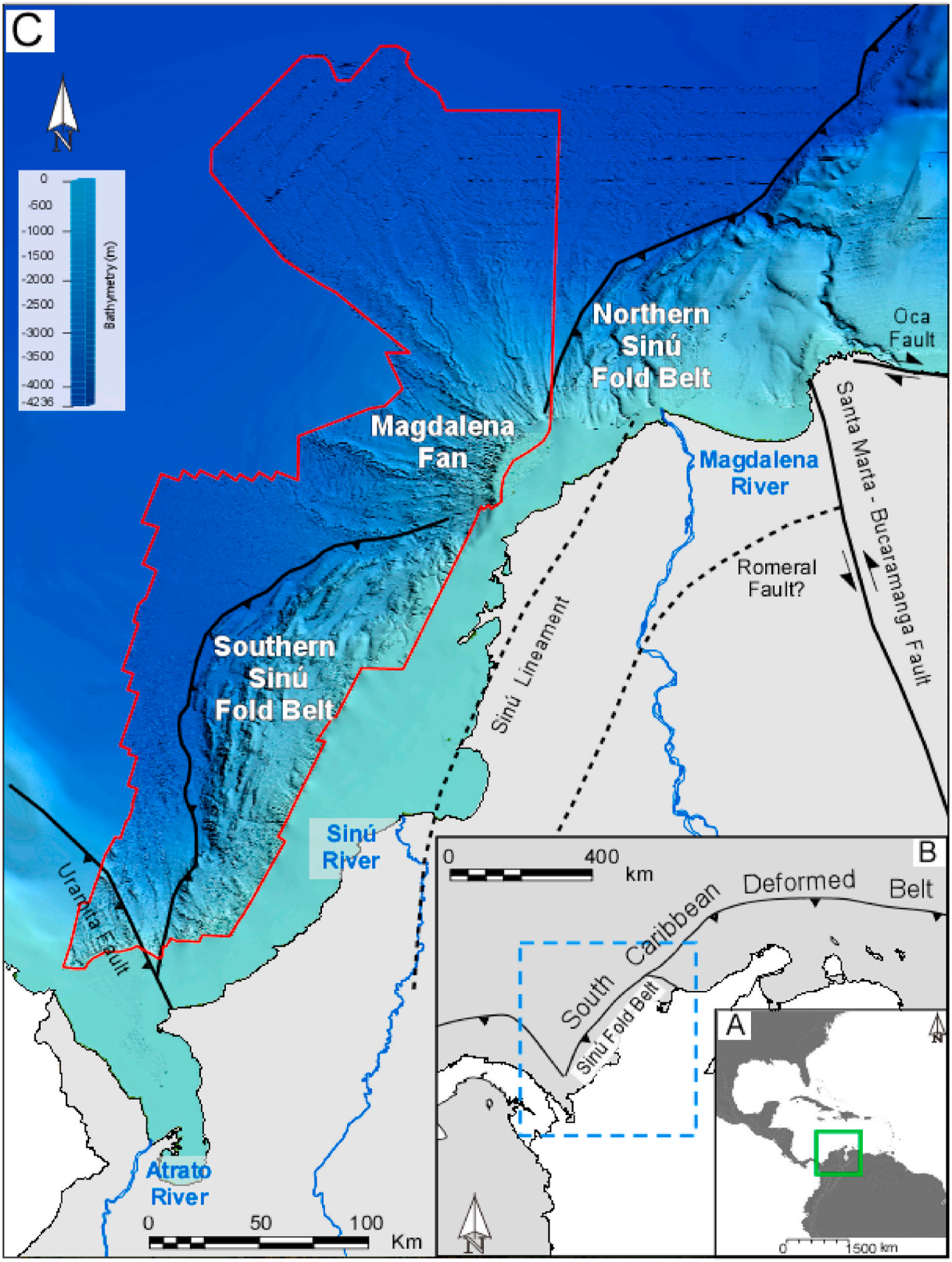

Fig. 1. Study area of the southern Caribbean of Colombia. (A) Schematic of the northern portion of South America, Central America, and the southern part of North America. Inset green box shows the location of part B. (B) Plate tectonic map of the South Caribbean Deformed Belt and Sinú Fold Belt, from Symithe et al. (2015) and Martinez et al. (2015). Inset blue box shows the location of part C. (C) Bathymetry map shows the seafloor topography created by tectonic deformation and sedimentation. Note the location of the Northern Sinú Fold Belt, Magdalena Fan and Southern Sinú Fold Belt. Faults traces are based on Ruiz et al. (2000) and Galindo and Lonergan (2020). Bathymetry data inside red polygon is multibeam data supplied by Ecopetrol S.A., and other data is provided by the GEBCO model. (For interpretation of the references to colour in this figure legend, the reader is referred to the Web version of this article.)

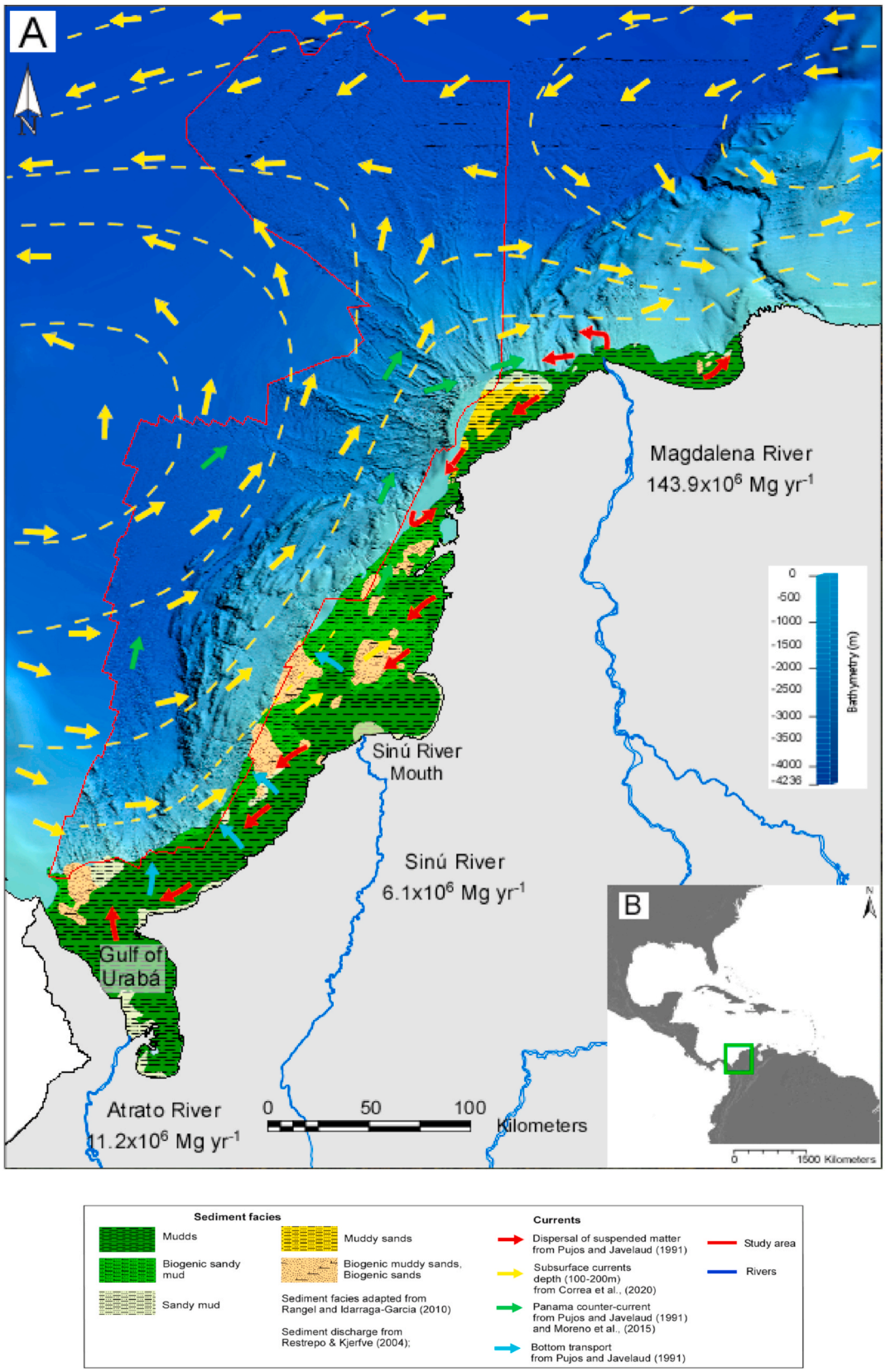

Fig. 2. Location of the three main rivers within the study area: The Magdalena, Sinú and Atrato rivers. Offshore sediment facies adapted from (Rangel-Buitrago and Idárraga-García, 2010) and surface and bottom currents based on Pujos and Javelaud (1991), Correa-Ramirez et al. (2020) and Moreno-Madriñán et al. (2015). The sediment discharge data from Restrepo and Kjerfve (2004). Inset B shows the location of part A. Bathymetry data inside red polygon is multibeam data supplied by Ecopetrol S.A., and other data is provided by the GEBCO model. (For interpretation of the references to colour in this figure legend, the reader is referred to the Web version of this article.)

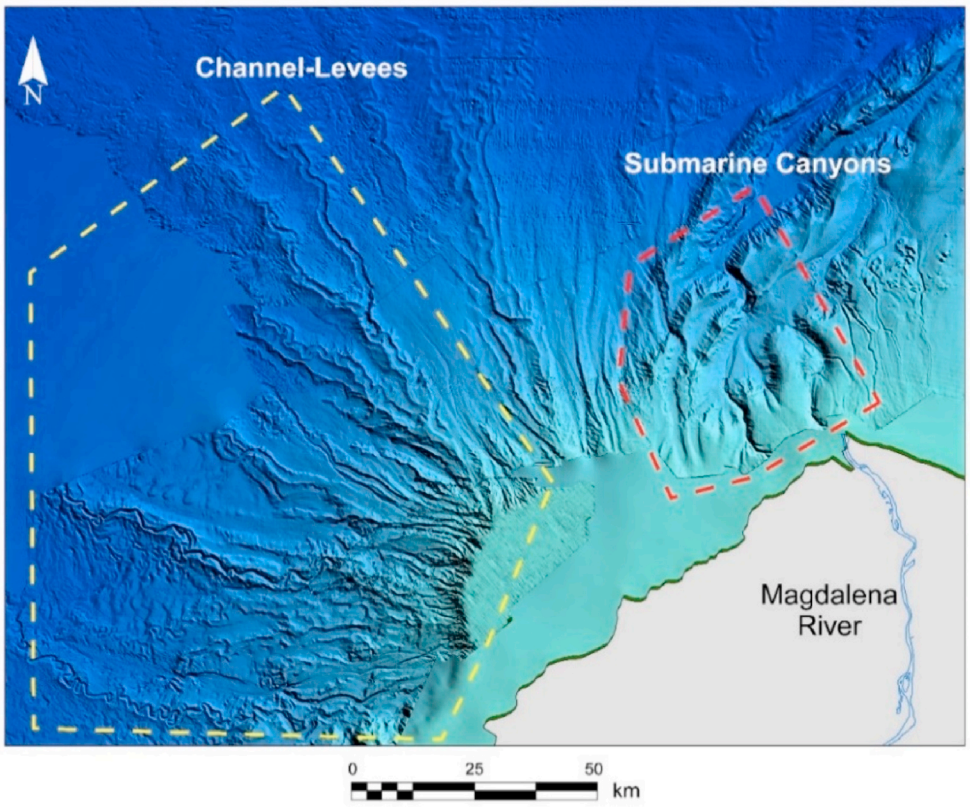

Fig. 3. Bathymetry showing the sea-bed morphology of the Magdalena Fan. The red box shows submarine canyons close to present-day Magdalena River mouth indenting the shelf edge; the yellow box highlights channel-levee systems that evolved in the zone of transition between the continental shelf and the continental slope. These channel-levee systems are currently inactive and are interpreted to have formed in the Pliocene-Pleistocene, before the Magdalena river mouth migrated northward to its present-day position (Romero-Otero et al., 2015). The bathymetry corresponds to the merge of the GEBCO model and the multibeam data supplied by Ecopetrol S.A. (For interpretation of the references to colour in this figure legend, the reader is referred to the Web version of this article.)

systems, but also, from erosive processes on the slope, mainly comprising the erosion of steep anticlinal crests and mass failures from over-steepened topography (Mutti, 1985; Posamentier and Walker, 2006; Shanmugam, 2016).

The southern Caribbean Colombian margin is a tectonically-active, convergent margin with high sediment supply, fed to the coastline by three major fluvial systems with marked differences in sediment supply: the Atrato, Sinú, and Magdalena rivers (Restrepo and Kjerfve, 2004, Fig. 1). The width of the shelf, which varies along strike, is also is a factor influencing sediment delivery into the offshore basin. Submarine channels, canyons, and landslides all transport sediments downslope, depositing sediment aprons that act to smooth the irregular tectonically-modified submarine landscape (Idárraga-García et al., 2019; Idárraga-García and Vargas, 2014; Morley and Leong, 2008; Ortiz-Karpf et al., 2015; Pettinga and Jobe, 2020; Pirmez et al., 2000; Romero-Otero et al., 2015; Sinclair and Tomasso, 2007; Vinnels et al., 2010).

In this study, we analyze the distribution and architectures of the deep-water gravitational deposits in the southern Colombian Caribbean, by integrating new multibeam bathymetry and 3D seismic data that cover a larger area than previous studies (Alfaro and Holz, 2014; Ercilla et al., 2002a; Estrada et al., 2005; Idárraga-García et al., 2019; Idárraga-García and Vargas, 2014; Kolla and Buffler, 1984a; Martinez et al., 2015; Ortiz-Karpf et al., 2017; Romero-Otero et al., 2015; Vinnels et al., 2010). We utilize these data to document the variability on the distribution and morphology of deep-water depositional elements in three areas that have variable boundary conditions (e.g., sediment supply, shelf width). We discuss the impacts of sediment supply, slope profile and shelf width on the evolution of seafloor topography, and propose a predictive model for assessing the interplay between these factors.

2. Study area

2.1. Geotectonic setting

The southern Colombian Caribbean is located, along the northwestern margin of South America (Fig. 1A). The geological evolution of northwestern South America is linked to the subduction of the Caribbean oceanic plate beneath the continental South American plate, which began in the late Cretaceous and continues today (Barat et al., 2014; Bernal-Olaya et al., 2015; Cortés and Angelier, 2005; Escalona and Mann, 2011; Flinch et al., 2003; Spikings et al., 2015; Taboada et al., 2000). Currently, the Caribbean plate maintains an eastward motion relative to the South American plate (Symithe et al., 2015). The oblique convergence of these two tectonic plates has created the South Caribbean Deformed Belt (SCDB) offshore of northern Colombia and Venezuela (Fig. 1B, Bernal-Olaya et al., 2015; Escalona and Mann, 2011). The SCDB displays a convex plainview shape that causes along-strike variations in the structural styles (Galindo and Lonergan, 2020). The southern area of the SCDB corresponds to the Sinú Fold Belt, a late Cenozoic sedimentary accretionary prism that is constrained to the east by the Sinú lineament (Duque-Caro, 1990, 1979; Martinez et al., 2015; Ruiz et al., 2000). Uplift and deformation began during late Cenozoic and continues at present (Bernal-Olaya et al., 2015; Cediel et al., 2005; Corredor, 2003; Cortés and Angelier, 2005; Duque-Caro, 1990, 1979), with a main deformation stage that occurred during the Pliocene-Pleistocene, associated with the Andean Orogeny (Duque-Caro, 1979; Flinch et al., 2003; Ruiz et al., 2000). The Magdalena Submarine Fan, where the slope appears relatively undeformed, segments the Sinú fold belt into a Southern and a Northern portion (Fig. 1C, Martinez et al., 2015).

2.2. Sediment supply and oceanographic setting

The study area includes three major river systems that supply

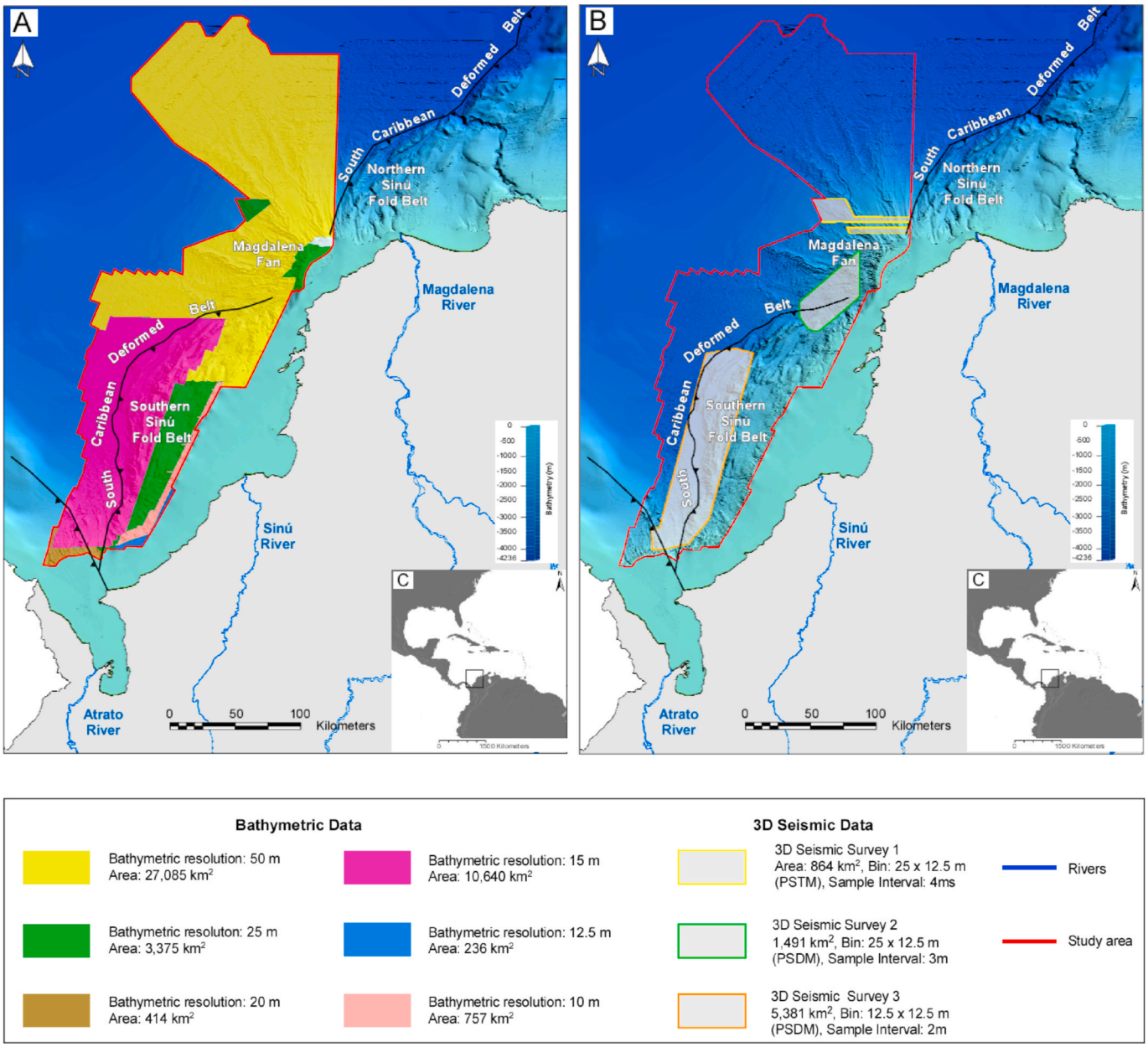

Fig. 4. Data available for this study. (A) Bathymetric surveys merged to build a regional seafloor topography with lateral resolutions from 10 to 50 m along the southern Sinú Fold Belt and Magdalena Fan. (B) 3D seismic surveys in the study area: 1) 3D seismic survey 1, located over the upper Magdalena Fan, 2) 3D seismic survey 2, over the area of transition between the Magdalena Fan and the Southern Sinú Fold Belt. 3) 3D seismic survey 3, located in the Southern Sinú Fold Belt. (C) Insets showing the location of (A) and (B) relative to northern South America. This high-quality regional data was provided by Ecopetrol S.A.

sediment from the continent: from north to south, the Magdalena, Sinú, and Atrato rivers. Additionally, terrigenous sediments are distributed over the shelf and slope by oceanic currents (Fig. 2, Correa-Ramirez et al., 2020; Moreno-Madriñán et al., 2015; Pujos and Javelaud, 1991).

The Magdalena River drains the northern portion of the Andean Cordillera (Fig. 2) and has the highest sediment discharge in the region, with 143.9 $\times$ 10^6 Mg yr^{-1} (Restrepo and Kjerfve, 2004). Close to the present-day Magdalena River mouth, the continental shelf width is very narrow, ~5 km (Fig. 3, Ercilla et al., 2002a, 2002b; Idárraga-García and Vargas, 2014; Idárraga-García et al., 2019; Kolla and Buffler, 1984a, 1984b). In this area, submarine canyons indent the shelf edge and transport sediments to the slope and the bottom of the basin (Romero-Otero et al., 2015). Toward the southwest of the Magdalena River mouth, the continental shelf is wider ranging from 15 to 32 km (Fig. 3). In this area, the main depositional systems are large channel-levee systems which evolve in the zone of transition between the continental shelf and the continental slope (Fig. 3, Ercilla et al., 2002a, 2002b; Idárraga-García et al., 2019; Kolla and Buffler, 1985; Romero-Otero et al., 2015). These channel-levee systems are currently inactive and are interpreted to have formed in the Pliocene-Pleistocene, before the Magdalena river mouth migrated northward to its present-day position (Romero-Otero et al., 2015).

The shelf sediments related to the present-day Magdalena River are predominantly mud and sandy-mud, including terrigenous and biogenic components (Fig. 2, Pujos and Javelaud, 1991; Rangel-Buitrago and Idárraga-García, 2010). These sediments are dispersed by the Panama counter-current towards the east of the Magdalena River mouth during the main wet season (September to November), but change direction during the dry season (December–February) to flow westward (Pujos and Javelaud, 1991). The regional subsurface currents also flow

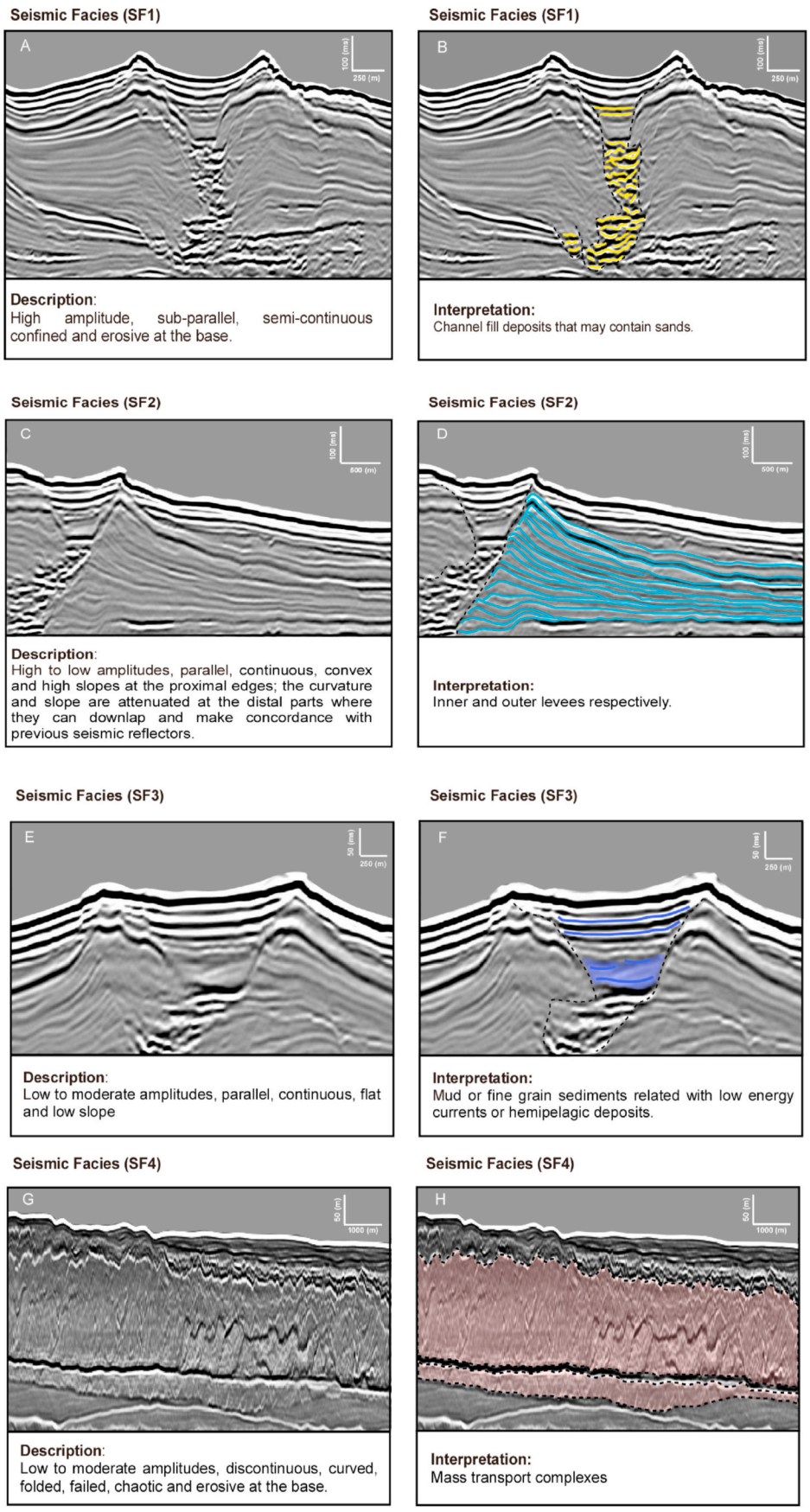

Fig. 5. Main seismic facies identified in this study (A, C, E, G, I, K, M) and interpretation (B, D, F, H, J, L, N).

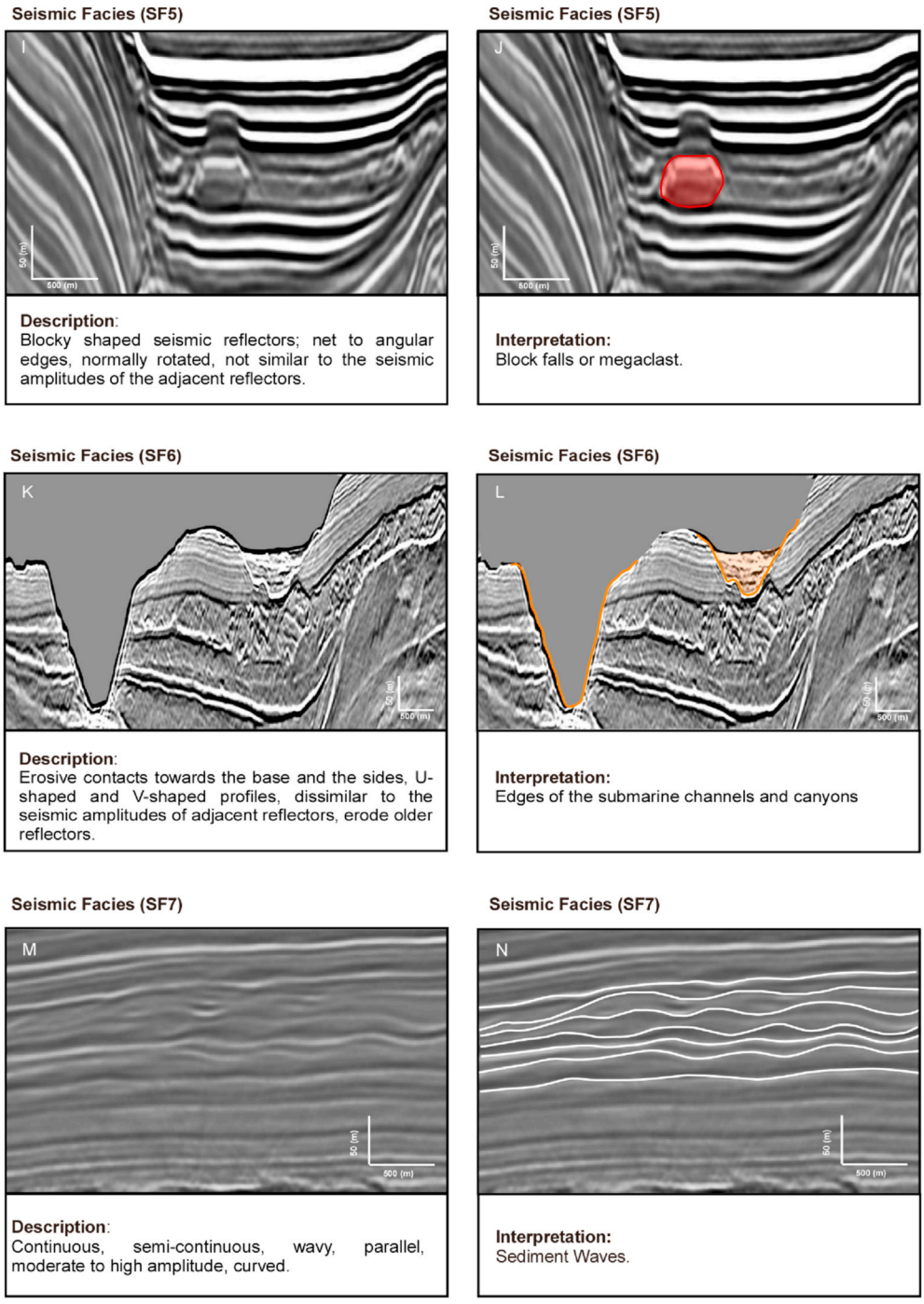

Fig. 5. (*continued*).

northeastward and eastward over the Magdalena Submarine Fan (Fig. 2, Correa-Ramirez et al., 2020).

South of the Magdalena, near the center of the study area, is the Sinú River (Fig. 2). It has the lowest sediment discharge among the three main rivers, with 6.1×10^6 Mg yr^{-1} (Restrepo and Kjerfve, 2004). The shelf width in this sector varies from 25 to 80 km (Vinnels et al., 2010). The sediments on the shelf are predominantly muddy (Fig. 2), although biogenic muddy sands also occur and are concentrated in mounds on the shelf (Pujos and Javelaud, 1991; Rangel-Buitrago and Idárraga-García, 2010). The sediment distribution during the wet season have a northeast trajectory, which is influenced by the Panama counter-current (Pujos and Javelaud, 1991). However, during the dry season, the distribution of suspended sediments is moved to the southward of the Sinú River delta mouth (Fig. 2, Pujos and Javelaud, 1991).

The third fluvial system, the Atrato River, is located in the southernmost part of the Colombian Caribbean margin, draining towards the Gulf of Urabá (Fig. 2). It has a moderate annual sediment flux of 11.2×10^6 Mg yr^{-1} (Restrepo and Kjerfve, 2004). The shelf width ranges between 24 and 113 km. The widest shelf is located in the Gulf of Urabá (~113 km), coincident with the location of the Atrato River delta, where sandy mud sediments are predominant (Fig. 2), while mud-sized sediments are predominant on the open shelf (Rangel-Buitrago and Idárraga-García, 2010). Sediment input from the river to the open shelf depends upon the circulation inside the Gulf of Urabá (Escobar and Velásquez-Montoya, 2018). In general, during the main dry season sediment transfer to the shelf is relatively low, and most sediment is

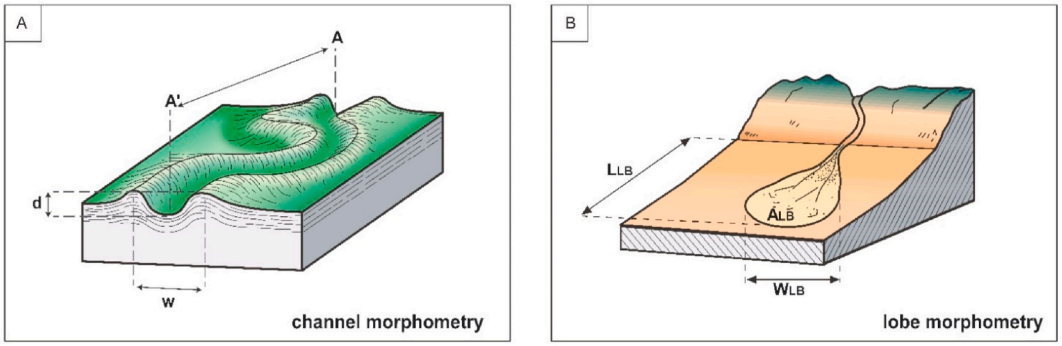

Fig. 6. Sketch of the morphometric parameters measured for channelized systems (A) and lobes (B). Channel depth, d, channel width, w, straight line joining the first point and the last midpoint of channel (section A-A′), lobe width, W_{LB}, lobe length, L_{LB}, and lobe area, A_{LB}. Methodology follows Shumaker et al. (2018) for channels and Pettinga et al. (2018) for lobes.

deposited inside of the Gulf of Urabá, while during the main wet season the increase of river input produces an outward flux of sediments, allowing transfer to the open shelf (Escobar et al., 2015; Pujos and Javelaud, 1991).

3. Methodology

This study analyzed approximately 7736 km^2 of 3D seismic and 42,500 km^2 of high-resolution bathymetric data along the southern Sinú Fold Belt and the southern Magdalena Fan (Figs. 1 and 4).

Ten different bathymetric surveys with lateral resolutions from 10 to 50 m were merged to build a regional seafloor topography (Fig. 4). Additionally, three 3D seismic reflection surveys covering the southern part of the Magdalena Fan and the Southern Sinú Fold Belt were integrated with the bathymetric data. 3D seismic survey No. 1, is located over the appex Magdalena Fan, and corresponds to a time-migrated volume, with a bin spacing of 25 × 12.5 m, and 4 ms vertical sampling rate; the average frequency is 40 Hz (Fig. 4). 3D seismic survey No. 2, is located in the area of transition between the Magdalena Fan and the Southern Sinú Fold Belt, and is a Post Stack Depth Migrated (PSDM) volume, with a bin spacing of 12.5 × 12.5 m and 3 m vertical sampling rate, the average frequency is 30 Hz. Finally, 3D seismic survey No. 3, is located over the area of the Southern Sinú Fold Belt, and corresponds to a PSDM volume, with a bin spacing of 12.5 × 12.5 m, and 3 m vertical sampling rate; the average frequency is 65 Hz. This study focuses in the interval between the seafloor surface and approximately 1 km below the seafloor. Seismic attributes and horizon slices were used to complement the description and interpretation of seismic facies and sedimentary bodies. These high-quality regional data were provided by Ecopetrol S. A.

3.1. Interpreted seismic facies

Seven seismic facies were identified in the 3D seismic (Fig. 5):

1) Seismic facies-1 (SF1), characterized by sub-parallel, semi-continuous, high-amplitude reflectors, confined within a basal surface that has an erosive base, and is interpreted as high-energy, sand-prone channel-fill deposits (Fig. 5A and B, 10, and 11, Abreu et al., 2003; Armitage et al., 2012; Jobe et al., 2015; Posamentier and Kolla, 2003).
2) Seismic facies-2 (SF2), composed of parallel, continuous, seismic reflectors with variable amplitudes. Occurring at either side of SF1, reflectors are convex and inclined away from SF1, curvature and slope are attenuated, and reflectors downlap underlying seismic reflectors. This seismic facies is interpreted as proximal and distal levees respectively (Fig. 5C and D, 10, 11, 21 and 22, Armitage et al., 2012; Deptuck et al., 2003).
3) Seismic facies-3 (SF3) contains continuous, parallel, horizontal reflectors with low to moderate amplitudes. Facies 3 is contained within a convex downward shape and is interpreted as low-energy, mud-prone channel-fill deposits (Fig. 5E and F, 10, 11, 12, 17, and 18 Prather et al., 1998).
4) Seismic Facies-4 (SF4) is composed of discontinuous, curved, folded, chaotic seismic reflectors with low to moderate amplitudes, typically overlying an erosive base. This seismic facies is interpreted to be imaging subaqueous mass failure deposits and complexes (Fig. 5G and H, 10, 11, 16, 17, 18, 19, and 22, Moscardelli et al., 2006; Moscardelli and Wood, 2008).
5) Seismic facies-5 (SF5) is composed of discrete packages of parallel seismic reflectors with sharp lateral terminations. These packages are commonly different in internal character and rotated with respect to adjacent seismic packages. This seismic facies is interpreted as blocks derived from gravitational collapse of anticlinal ridges and basin walls, and canyon margins (Fig. 5I and J, 17 and 21, Gamboa et al., 2011; Jackson, 2011).
6) Seismic facies-6 (SF6) is characterized by seismic reflectors are confined within U-shaped and V-shaped concave eroded features, and that lap out or thin onto the margins of these containers. These seismic facies are interpreted to filling submarine channels and canyons that erode the seafloor (Fig. 5K, L, 10, 11, 18, 21 and 22, Jobe et al., 2011).
7) Seismic facies-7 (SF7), is composed of continuous, semi-continuous, wavy, parallel reflectors with moderate to high amplitudes. This seismic facies is interpreted as sediment waves (Fig. 5M, N and 18, Faugères and Mulder, 2011; Posamentier and Kolla, 2003).

3.2. Morphometry of deep-water gravitational deposits

To analyze the morphometry of channels, canyons and lobes, we followed the methodology proposed by Shumaker et al. (2018) and Pettinga et al. (2018). We measured the depth of channelized system (*d*) as the vertical distance between the deepest point of the channel and the highest point of the levee crests (Fig. 6). The channel margins defined as the highest points of the crests of its channel borders. The width of the channel (*w*) was measured perpendicular to the thalweg line and it corresponded to the distance between the two channel margins (Fig. 6). We calculated the sinuosity by dividing the length of the channel along the thalweg (channel axis) by the distance of a straight line joining the first point and the last midpoint. Each measurement was then tabulated and reported in percentiles for each channel (P_{10} and P_{90}). For quantification of submarine lobes (Fig. 6), maximum lobe width (W_{LB}), maximum lobe length (L_{LB}) and lobe area (*ALB*) were measured following the methodology of Pettinga et al. (2018).

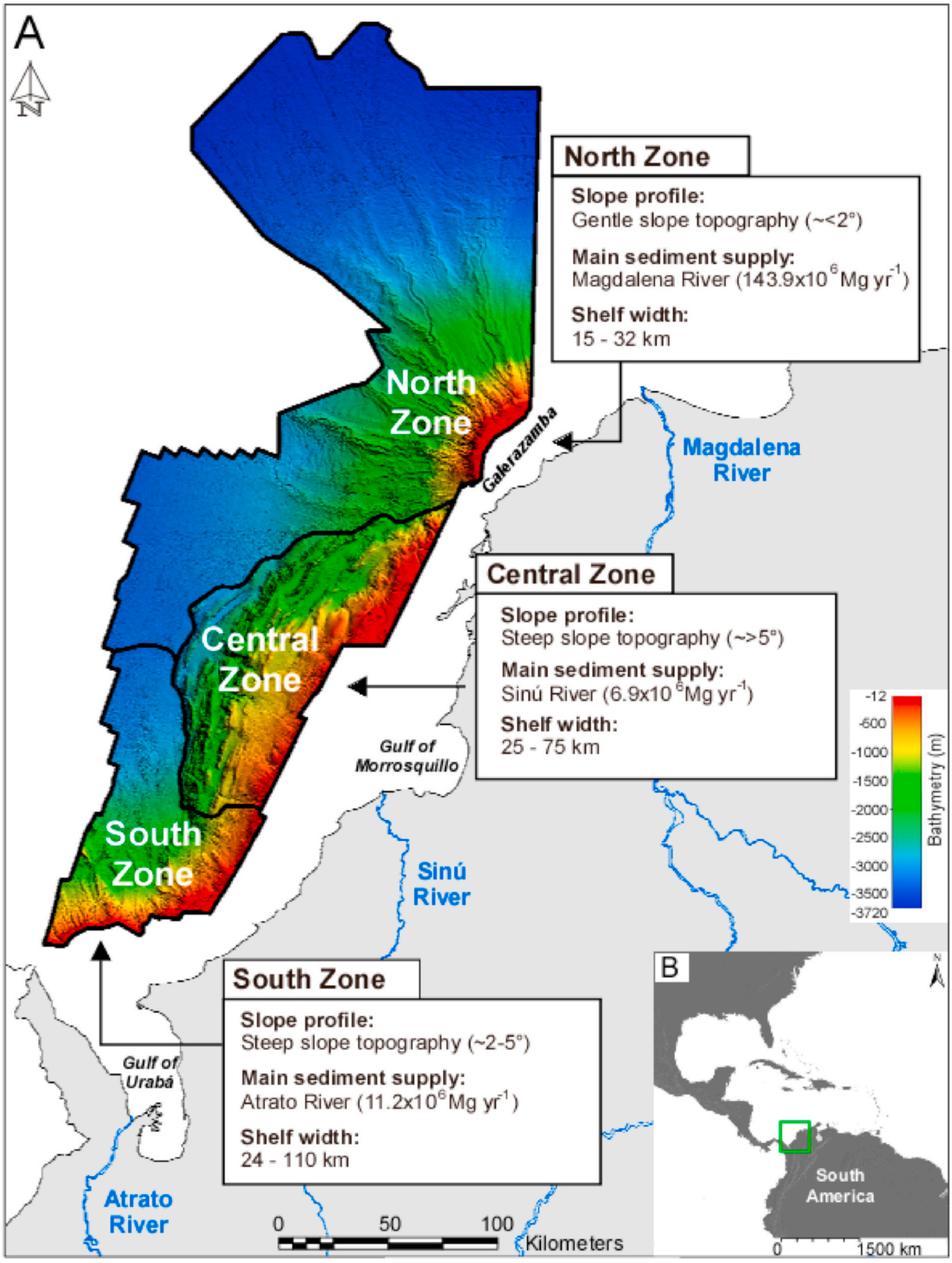

Fig. 7. Geomorphological zones in the area of study. The Northern Zone is associated with sediment input from Magdalena River. The Central Zone is mainly fed by the Sinú River. The Southern Zone is fed by the Atrato River. Each zone has a unique distribution and architecture of deep-water gravitational deposits. (B) Insets showing the location of (A) relative to northern South America. Sediment discharge data from Restrepo and Kjerfve (2004).

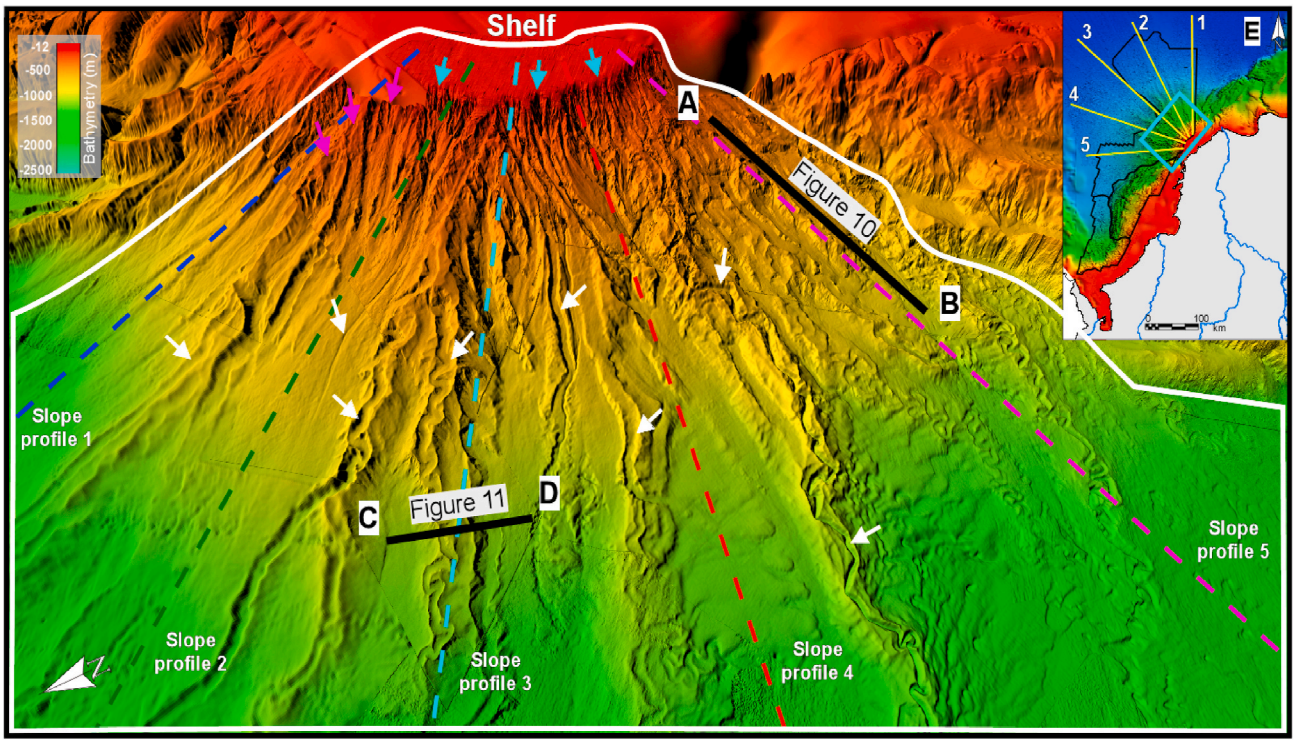

Fig. 8. 3D Bathymetric image of channel-levee systems in the Northern Zone. Channels start as gullies (light blue arrows), which merge downslope to become channel-levee systems (white arrows). Most channels do not impinge upon the shelf edge. E) Insets showing the location of Fig. 8 (light blue box) and slope profiles of Fig. 9 (yellow lines), relative to southern Caribbean region of Colombia, South America. (For interpretation of the references to colour in this figure legend, the reader is referred to the Web version of this article.)

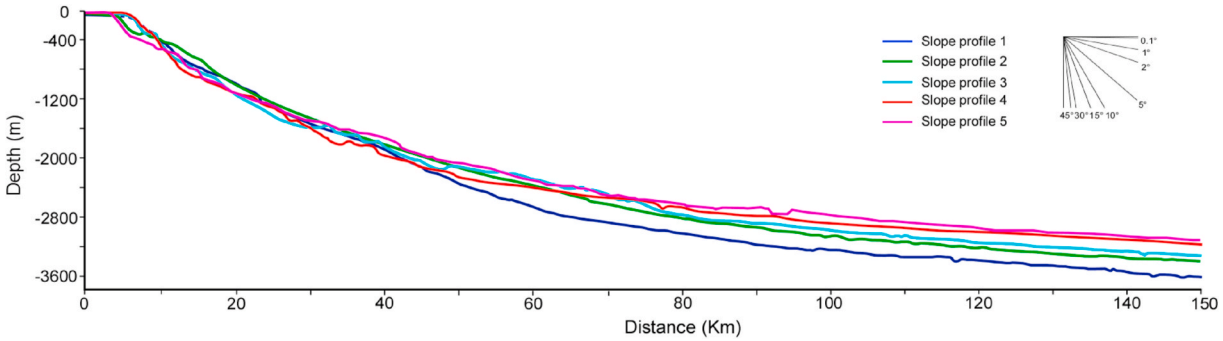

Fig. 9. Slope profiles through the Northern Zone. Slopes are overall gentle, with values ~ <2°. Note that towards the zone of transition between the continental shelf and the slope, gradients increase to ~5° and then gently decrease in the stream-wise direction. Location of profiles are shown in Fig. 8.

4. Results

Based on the data collected we propose that the study area can be divided into three geomorphological zones (Fig. 7) with unique sediment dispersal patterns and depositional architectures.

4.1. Northern Zone (Magdalena Fan)

The Northern Zone (Figs. 7 and 8) is an area characterized by high sediment supply from the Magdalena River (Restrepo and Kjerfve, 2004). Here, the continental shelf varies in width from 15 to 32 km. In the area of Galerazamba, the Northern Zone is dominated by the presence of extensive channel-levee systems with lengths that can exceed 150 km (Figs. 7 and 8, Ercilla et al., 2002a; Estrada et al., 2005; Idárraga-García et al., 2019; Romero-Otero et al., 2015). This zone is also characterized by a gentle slope (Fig. 9, ~ <2°). Toward the southwestern of the Galerzamba area, thrust faults and folds have been eroded and covered by the high volumes of sediment provided by the Magdalena River, smoothing the seafloor topography (Figs. 7 and 10). These channels are intepreted to have been active mainly during the Pliocene-Pleistocene (Romero-Otero et al., 2015).

In the Northern Zone, channel-levee systems are predominantly aggradational (Fig. 11) and stack vertically for more than 350 m (cf. Jobe et al., 2016). Most channels do not impinge upon the shelf edge, and typically evolve in the zone of transition between the continental shelf and the toe of the continental slope. Channels start as gullies, which merge downslope to become channel-levee systems (Figs. 8 and 12). The channel systems mainly trend northwest, and less commonly towards the southwest (Fig. 7). The channels show a reduction in depth from the slope to the basin floor. On the slope, the channel depths range from 14 to 125 m (P_{10} to P_{90} values). Once the channels reach the basin floor, channel depth decreases rapidly to values between 10 and 29 m. Channel widths are more stable, with values from 736 to 2354 m on the slope decreasing to 877 to 1783 m on the basin floor. The sinuosity

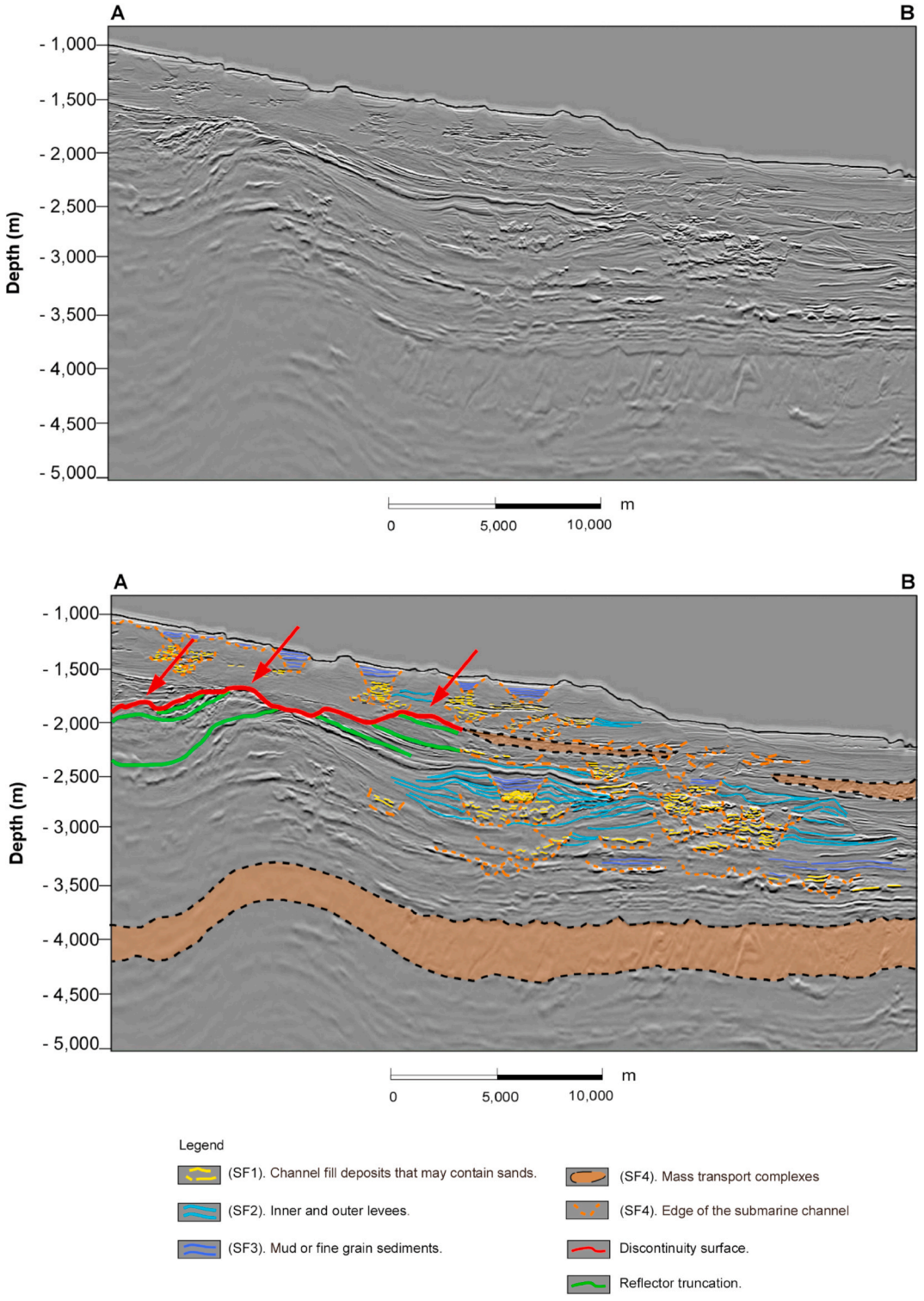

Fig. 10. Seismic profile along the Northern Zone. Upper image is uninterpreted. Lower image is interpreted, identifying principle seismic facies. Thrusts and folds are eroded by gravity flows (red arrows). Erosional scours are healed by sediments provided by the Magdalena River resulting in a smoothing of the seafloor topography (See Fig. 8 for Location). (For interpretation of the references to colour in this figure legend, the reader is referred to the Web version of this article.)

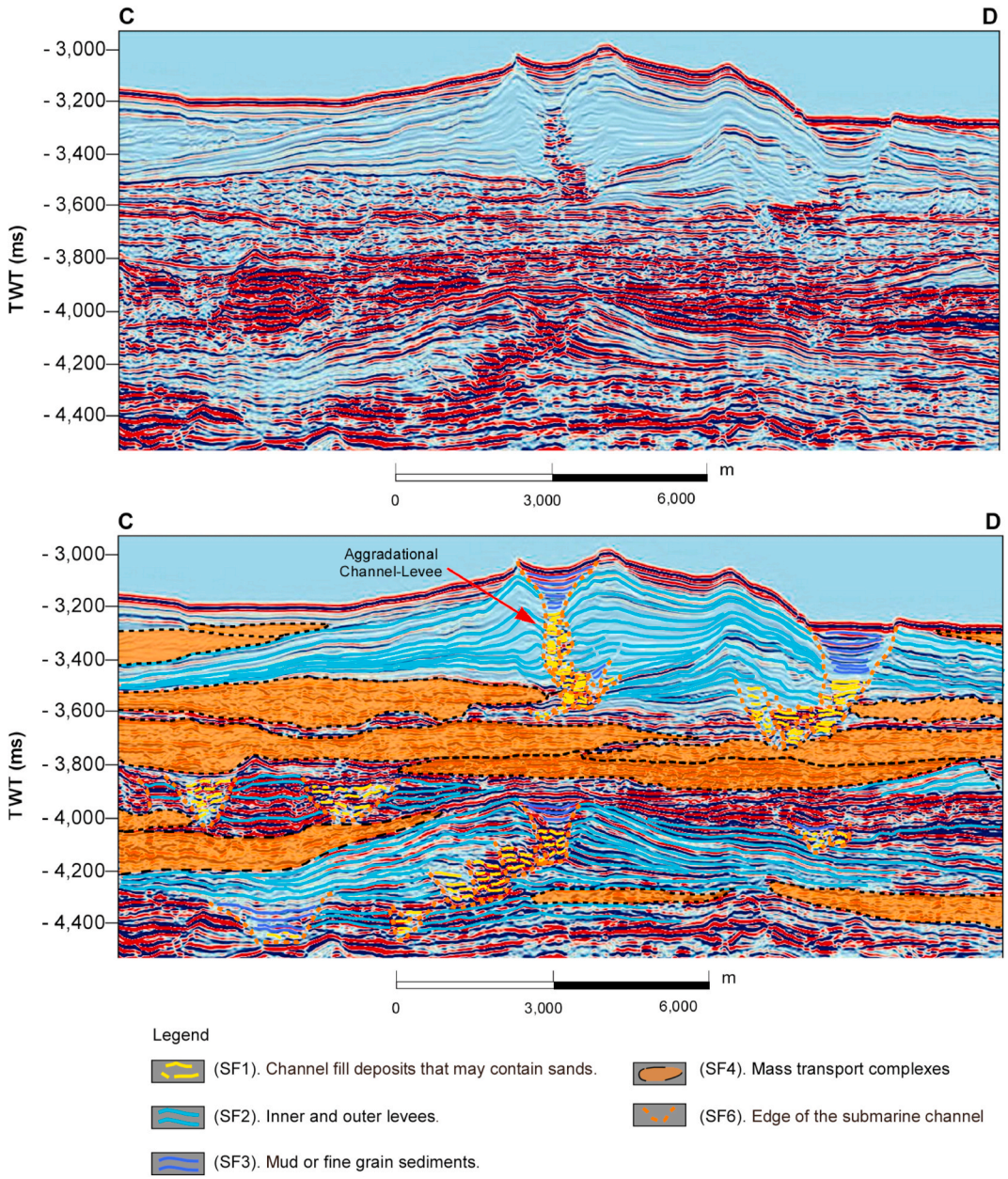

Fig. 11. Seismic profile showing the main seismic facies identified in the Northern Zone. Channel levee systems stack vertically for more than 350 m in the Northern Zone, reflecting the high rates of sediment supplied from the Magdalena River (See Fig. 8 for Location).

varies between 1.2 and 1.6 and tends to increase towards the lower slope and basin floor.

In the Northern Zone, mass-transport complexes (MTCs) are common (Figs. 11 and 12). The larger deposits are commonly associated with mass failures starting near the edge of the shelf, the flanks of channel-levees and gullies where slopes exceed ~5° (Figs. 9 and 12, Idárraga--García et al., 2019; Idárraga-García and Vargas, 2014; Ortiz-Karpf et al., 2016; Romero-Otero et al., 2015). These failures translate along bathymetric lows created between external levees, or along channel-levee systems, smoothing the seafloor topography (Ortiz-Karpf et al., 2017). Here, submarine mass failures are important agents that modify the slope, creating or closing sediment-flow pathways and thus modifying the architecture of the Magdalena fan (Idárraga-García et al., 2019; Idárraga-García and Vargas, 2014; Ortiz-Karpf et al., 2016; Romero-Otero et al., 2015).

4.2. *Central zone*

The central zone is the most structurally deformed part of the study area (Figs. 7 and 13). It contains northeast-southwest trending anticlines with steep flanks and piggyback sub-basins that form a rugose slope profile (Fig. 14). This zone is sediment-starved relative to the Northern Zone, only receiving sediment supplied by the Sinú River. The continental shelf width of the Central Zone varies between ~25 and 75 km (Fig. 7).

In the Central Zone, submarine canyons are the main conduits for basinward sediment transport. Canyons start as gullies on the upper continental slope, which merge downslope to form wider, erosive submarine canyons through which sediments travel basinward (Fig. 15). Near their points of initiation, gullies vary in width from 532 to 1,311m and in depth from 32 to 119 m (P_{10} to P_{90} values). Canyons vary in width between 607 and 2811 m, and in depth between 61 and 316 m. Average sinuosities are below 1.2 (lower than the channel-levee systems in the

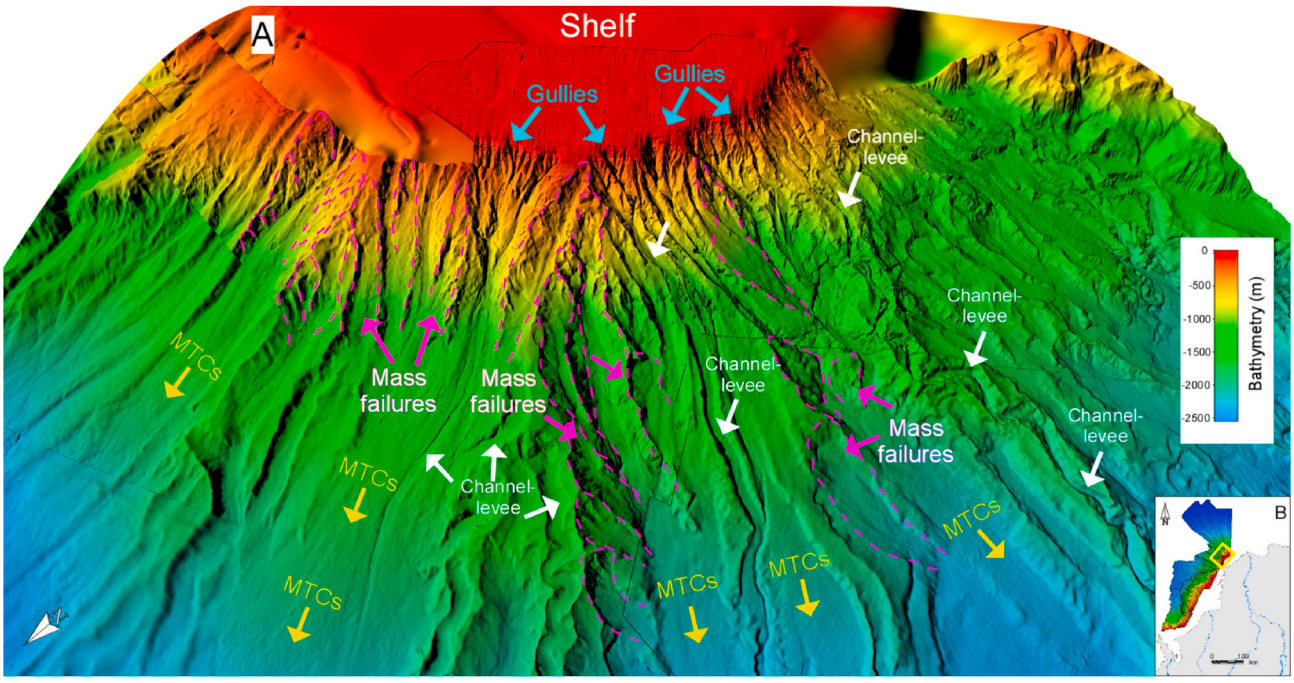

Fig. 12. (A) Detailed 3D bathymetric image in the Northern Zone showing erosional scours created by mass failures near the edge of the shelf and associated with steeper channel-levee and gully flanks (~5°). These remobilized sediments are deposited as mass-transport complexes (MTCs). (B) Insets showing the location of (A) relative to southern Caribbean of Colombia.

Northern Zone). The thalweg slope of these canyons is spatially variable, with canyons that exhibit high slopes (values over 20°) when crossing thrusts folds, and lower slopes across piggyback sub-basins (values lower than 1°). Flows traveling along some canyons erode the forelimbs of the anticlines, resulting in the interconnection of two or more piggyback sub-basins (Fig. 13). Moreover, erosion along the canyon thalwegs can reduce slopes to <5°. Upon reaching the piggyback sub-basins and basin floor, canyons lose confinement and can evolve geomorphologically into submarine channels or lobes (Figs. 15 and 16).

In the Central Zone, fold limbs form steep seafloor slopes (7–22°), which are prone to mass wasting (Fig. 13, Idárraga-García and Vargas, 2014; Vinnels et al., 2010). These failures generate block falls with individual blocks reaching maximum sizes of ~450 × 268 m (Fig. 17) and detached mass-transport complexes (*sensu* Moscardelli and Wood, 2008), which commonly run out less than 15 km from their sites of initiation. When the thrust-cored anticlines are not breached by submarine canyons, they act as topographic barriers for the movement of sediment, resulting in areas basinward of these barriers where sediment waves are preserved (Fig. 18).

4.3. Southern Zone (southern sinú fold belt)

The Southern Zone (Figs. 7, 19 and 20) is mostly composed of SF4, interpreted as mass transport complexes (Fig. 21, MTCs). These MTCs produce failure scars that can be traced to the upper continental slope, just below the shelf edge (Fig. 19). In this zone, the seafloor has been greatly modified by mass wasting; anticlinal crests have been eroded and piggyback sub-basins filled, burying the thrust belt (Figs. 19 and 21). Mud volcanoes are present and associated with intense compressional deformation (Figs. 19 and 21, Alfaro and Holz, 2014; Ruiz et al., 2000).

In the Southern Zone, the continental shelf ranges in width between ~24 and 110 km. The widest shelf occurs in the Gulf of Urabá sector (~110 km), coincident with the location of the Atrato River delta (Fig. 7). Erosional scours carved on the seafloor by mass failures merge basinward to become submarine canyons (Fig. 19). These canyons do not head near the shelf edge (Fig. 19) and are significantly larger than those in the Central Zone, with widths that vary between 3978 and 7550 m, and their depths range between 75 and 278 m (P_{10} to P_{90} values).

In the Southern Zone, MTCs initiate as slope-attached mass failures (*sensu* Moscardelli and Wood, 2008) that are considerably larger than the detached failures seen in the Central Zone, with sizes up to 80 km long by 20 km wide, and thicknesses exceeding 200 m (Fig. 22).

5. Discussion

The distribution of deep-water gravitational deposits in the Colombian Caribbean margin is the result of the complex interaction between slope morphology, sediment supply and continental shelf width. Tectonic deformation creates highly irregular slope profiles that can be smoothed through erosion and sedimentation. In addition, shelf width influences the transfer and reworking of sediments from the river delta mouths to the slope, controlling the volume and particle size of the sediments reaching the shelf edge (Sømme and Jackson, 2013; Sweet and Blum, 2016). In the following sections we analyze the role of each of these parameters on the resulting depositional patterns.

5.1. Slope profile

Previous studies indicate that the slope profile exerts control on the distribution of deep-water gravitational deposits in the southern Caribbean of Colombia (Cadena et al., 2015; Idárraga-García and Vargas, 2014; Romero-Otero et al., 2015; Vinnels et al., 2010). Areas with steep slope profiles (>2–5°), often located near the shelf-slope break, on the flanks of anticlines, and on levee flanks, are prone to mass failures (Figs. 12, 13 and 19; e.g., Idárraga-García et al., 2019). Slope gradient also influences the development of channels and canyons (Deptuck et al., 2012; Shumaker et al., 2018). In the Central and Southern Zones, submarine canyons occur in areas dominated by steep slopes, close to the shelf edge and across the steep flanks of thrust-cored anticlines (>2–5°, Figs. 15, 19 and 20). On the other hand, submarine channels are related with areas of overall gentle slope topography (<2°, Figs. 8 and 9), also across piggyback sub-basins and on the bottom of the basin (<1°, Fig. 15). This relationship between slope gradient and the development of canyons and channels has been documented offshore of Angola

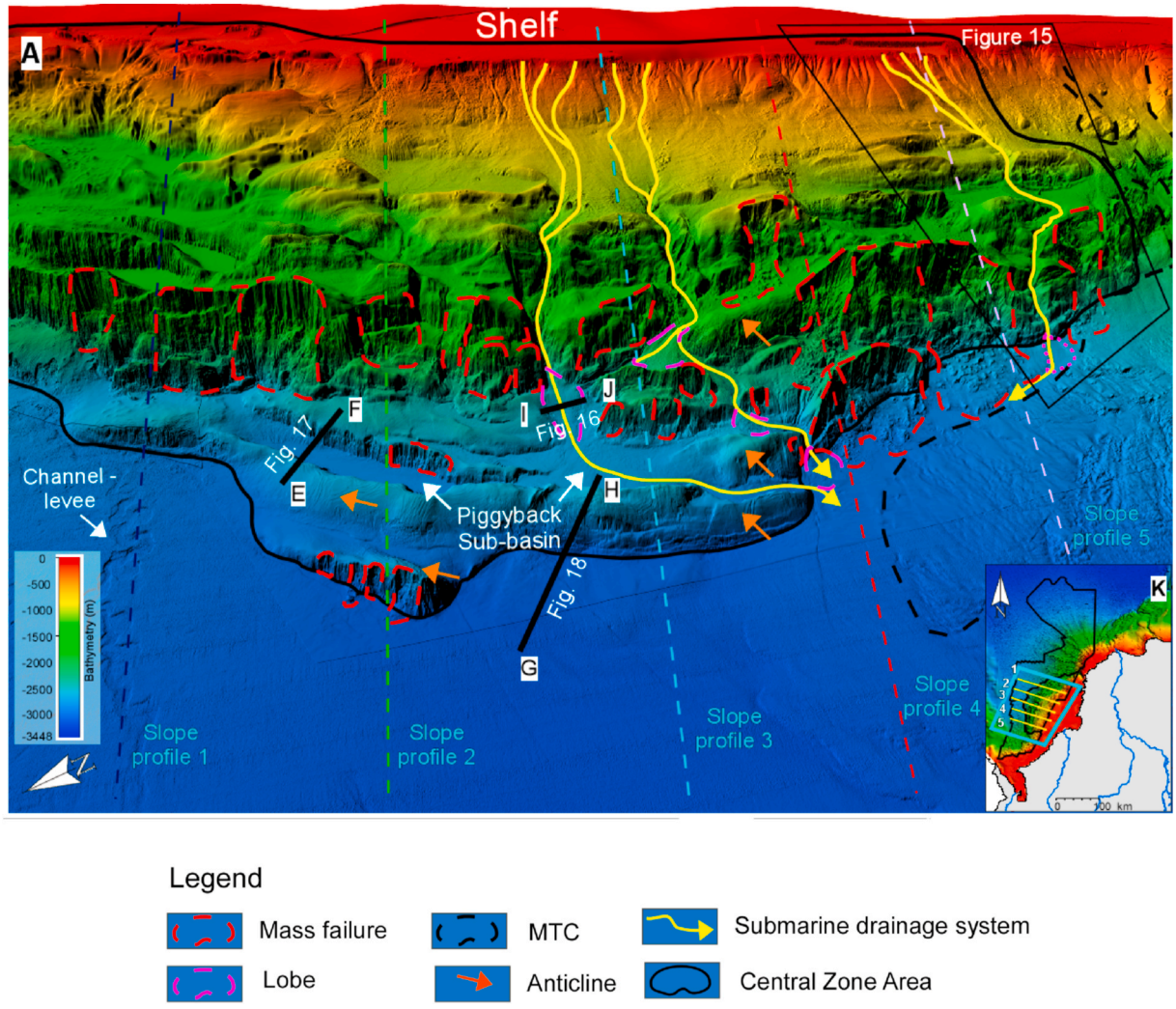

Fig. 13. Bathymetry 3D view of the Central Zone, highlighting mass failures and tortuous submarine drainage system related with anticline and piggyback sub-basins that create seabed topography and influence sediment distribution. Greens are high and blues are low elevations. Locations of slope profiles plotted in Figure- 15 and locations of Figs. 15–18.

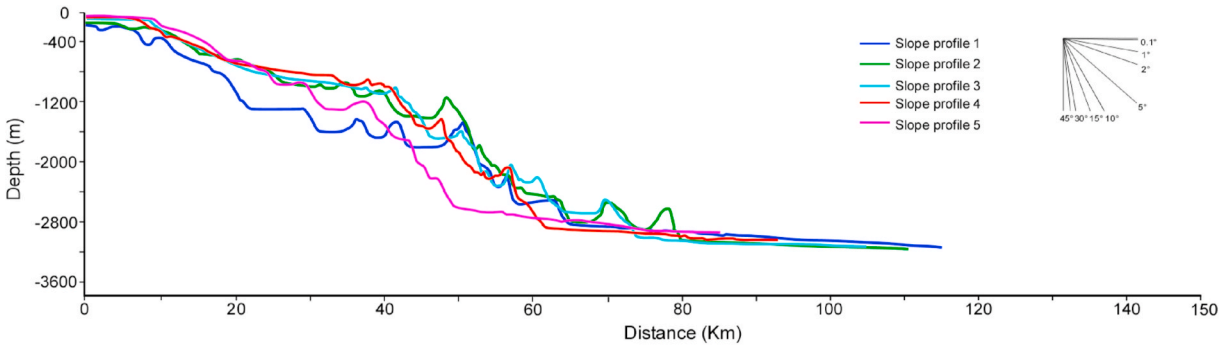

Fig. 14. Slope profiles through the Central Zone. The profile shows an irregular slope topography. Steep slopes (~>5°) are related with anticlines and lower slopes are associated to piggy-back sub-basins. The locations of the profiles are shown in Fig. 13.

(Oluboyo et al., 2014), also in the Eastern Mediterranean Sea and along the continental margin of Equatorial Guinea, where the structural deformation and slope profile exerts a strong control on channel location and evolution (Clark and Cartwright, 2009; Jobe et al., 2011). In the study area, channel sinuosity varies between 1.2 and 1.6 and tends to increase towards the lower slope (<2°, Idárraga-García et al., 2019; Romero-Otero et al., 2015). Submarine canyons exhibit low sinuosities (<1.2) that are less variable and likely related to erosion-dominated processes on these steep slopes.

5.2. Sediment supply

Continental sediment supply constitutes another key control on the distribution and morphology of deep-water deposits (Catuneanu, 2020,

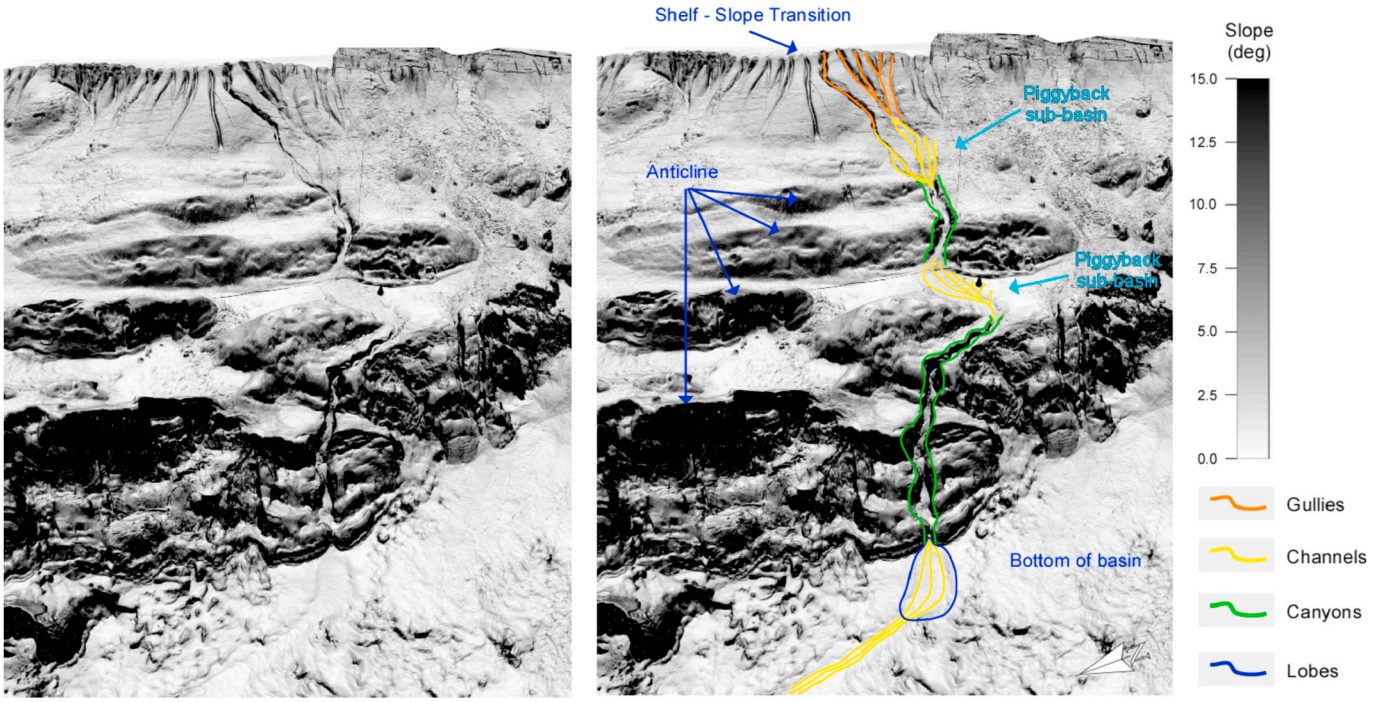

Fig. 15. Slope gradient 3D image showing the evolution of a drainage system from the upper slope to the bottom of basin in the Central Zone. Drainage systems start as gullies on the upper continental slope which merge downslope to form, submarine channels when crossing lower slopes across piggyback sub-basins, and canyons when passing through the structural thrusts with high slopes. Upon reaching the basin floor the canyons lose confinement and can evolve to submarine channels or lobes. See for location, black box in the upper right of Fig. 13.

2002; Jervey, 1988; Pettinga and Jobe, 2020; Prather, 2003, 2000). The anticlines and piggyback sub-basins developed by tectonic deformation can be degraded and filled by the high sediment fluxes along the southern Caribbean of Colombia (Figs. 10, 19 and 21). The smoothing of the slope gradient by sedimentation and mass failures enables direct transfer of sediments from the shelf break to the bottom of the basin (Figs. 12 and 19). When fine-grained, high sediment supply (>100 × 10^6 Mg yr^{-1}) occurs with a gentle slope gradient (<2°), large channel-levee systems can develop, as in the Northern Zone. The large volumes of fine-grained sediments accumulate in high-relief levees that confine the flows, allowing flows to travel downslope for hundreds of kilometers. A similar association between high sediment supply, gentle slope gradient, and the occurrence of extensive channel-levee systems occurs in the convergent margin of India, along the Bengal fan (Ma et al., 2020). Also, large channel-levee systems have been documented in the salt-diapir-influenced Fuji-Einstein system (Eastern Gulf of Mexico, Milliman and Meade, 1983; Piper et al., 2012; Sylvester et al., 2012), in the extensional domain of the upper- and mid-slope regions of the deep-water Niger Delta (Chima et al., 2019; Jolly et al., 2017) and in the Amazon Fan, (Pirmez et al., 2000; Pirmez and Flood, 1995).

Conversely, if high sediment supply occurs with a steep slope gradient, mass failures can occur frequently at the shelf edge, eroding, covering and smoothing the sea-floor topography as seen in the Southern Zone (Figs. 12 and 19). Finally, if low sediment supply coexists with a steep and irregular slope topography, even though the steep anticline flanks (7–22°) are prone to erosion and local detached mass failures (Figs. 13, 17 and 19, *sensu* Moscardelli et al., 2006), degradation of tectonic structures is less efficient. In this configuration, submarine canyons can incise the thrust-cored anticlines and allow the interconnection of two or more piggyback sub-basins, thus creating tortuous sediment pathways (Fig. 13, Smith, 2004; Vinnels et al., 2010). Upon reaching the piggyback sub-basins and the basin floor, canyons lose confinement and can evolve into submarine channels or lobes (Fig. 15, Oluboyo et al., 2014). Similar depositional architectures are also identified in the northwestern convergent margin of Borneo, where piggyback sub-basins and anticlines develop (Morley and Leong, 2008). This combination results in the creation of local detached mass failures and submarine canyons crossing the anticlines. In such settings, sediments tend to be trapped on the slope piggyback sub-basins, with only minor volumes reaching the bottom of the basin.

In the southern Caribbean region of Colombia, areas with low sediment supply and smooth slopes are absent. Such a setting has been documented west of Ireland in the southern Porcupine basin (Dorschel et al., 2010). There, sediment transfer from the shelf edge to the bottom of the basin occurs through the Gollum channels, which merge downslope to create wider submarine canyons (Dorschel et al., 2010). The morphology of the submarine channels in the Porcupine Basin is similar that of channels that develop in the Central Zone in areas of low slope gradients (<2) across the piggyback sub-basins (Fig. 15). This observation suggests that the type of sediment conduit that develops in any particular setting is greatly influenced by the interaction of the slope gradient and sediment supply.

5.3. *Shelf width*

The continental shelf width influences sediment transfer from the river delta mouths to the shelf edge (Sømme and Jackson, 2013; Sweet and Blum, 2016). In general, on wider shelves sediments tend to accumulate in the shallow marine environments, while narrow shelves deliver sediments more efficiently to deep-water environments (e.g., Catuneanu, 2020). In the southern Caribbean region of Colombia, areas with narrow shelves (<5 km) exhibit submarine canyons that deliver sediments directly from the river deltas to the slope (Fig. 3). These features are observed close to the present-day Magdalena River mouth (Fig. 3, Ercilla et al., 2002a, 2002b; Idárraga-García et al., 2019; Romero-Otero et al., 2015). Alternatively, in zones with wider shelves like the Southern Zone, most of the sediment transfer is related with bottom and surface shelf currents and is mainly fine grained (Fig. 2, Correa-Ramirez et al., 2020; Moreno-Madriñán et al., 2015; Pujos and Javelaud, 1991). Most of the coarser-grained sediments in the Southern

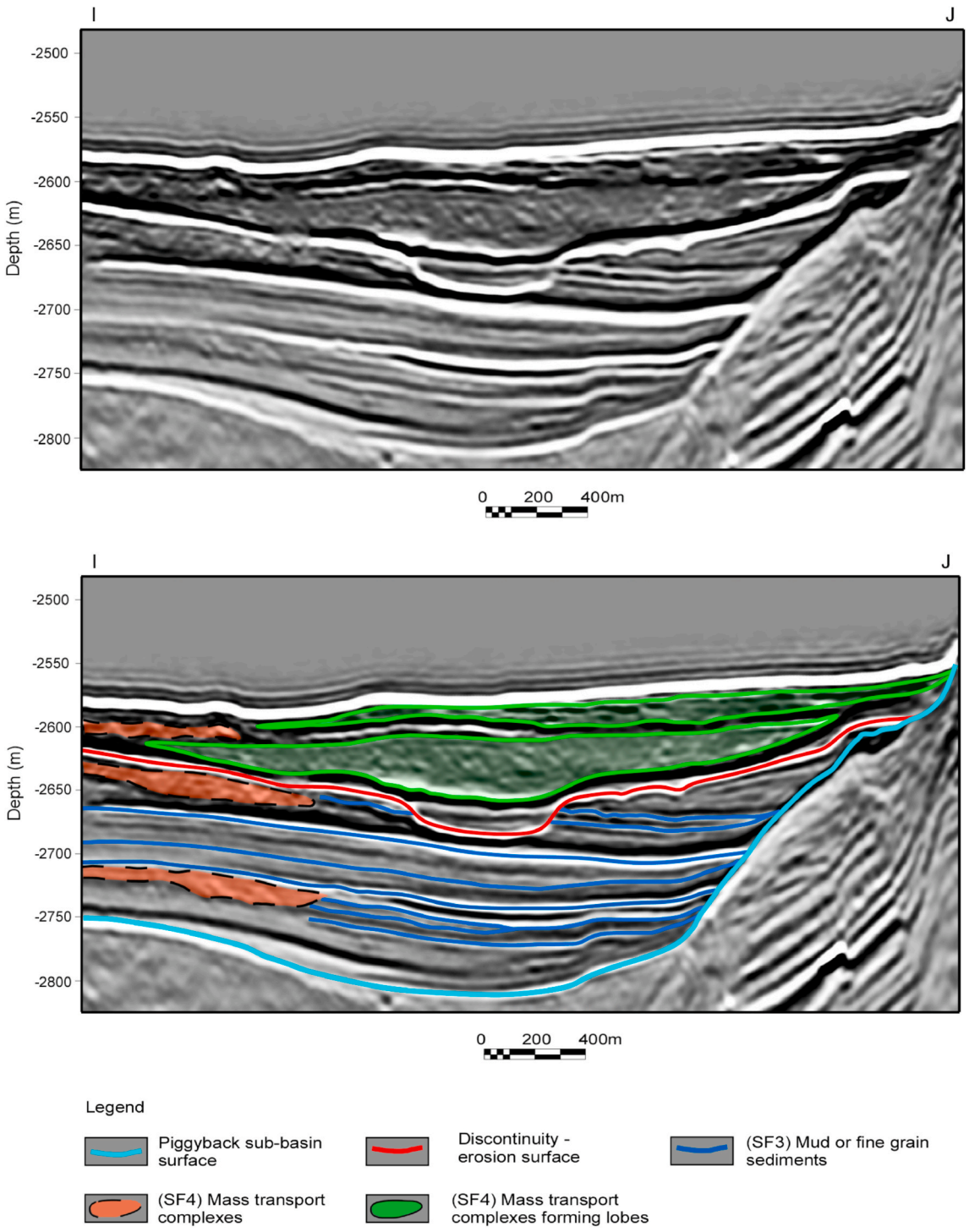

Fig. 16. Uninterpreted (upper) and interpreted (lower) seismic profile showing lobe-shaped mass transport complexes. These are fed by canyons and become unconfined upon reaching the piggyback sub-basins. Location of seismic line is given in Fig. 13 (I-J black line).

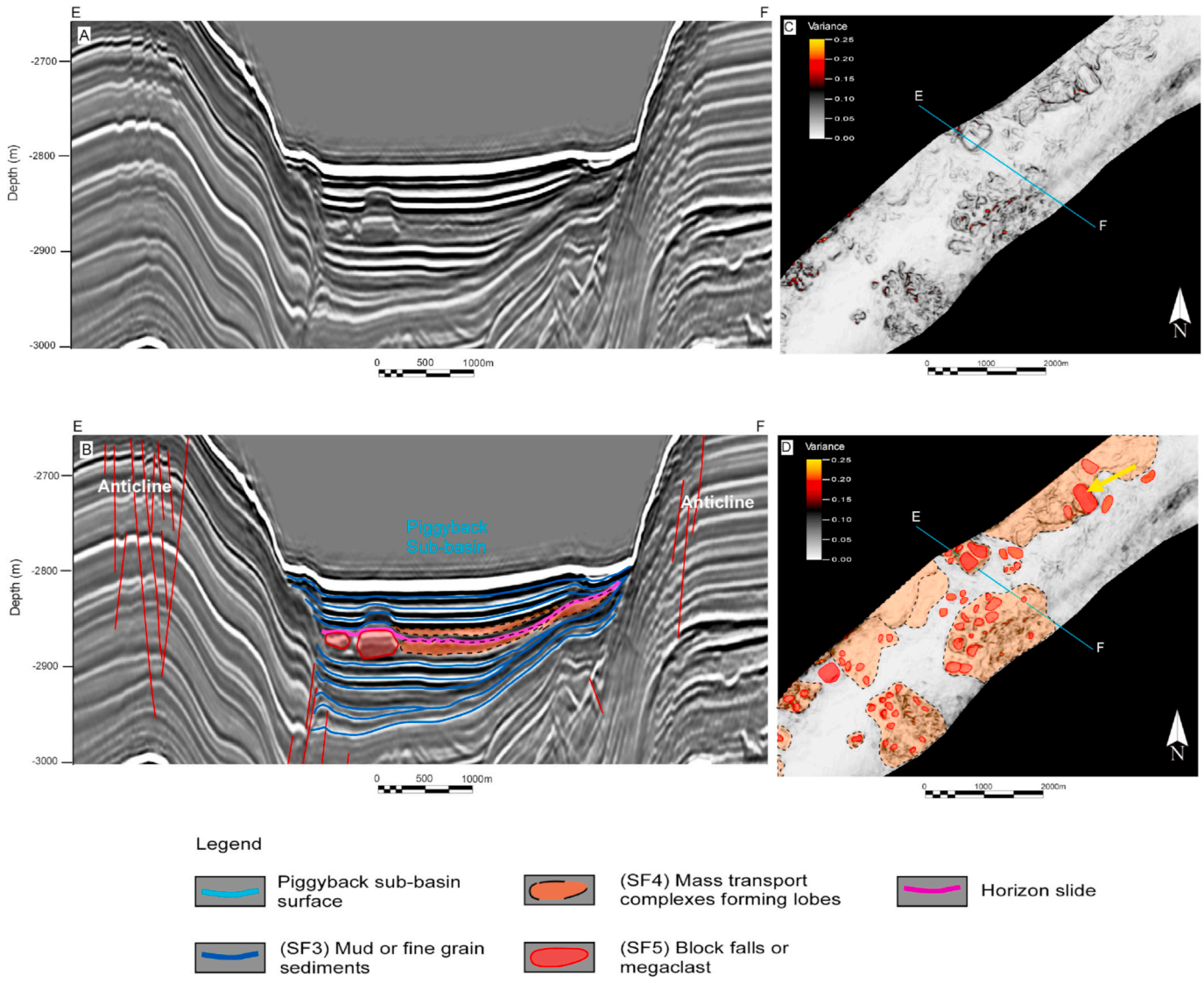

Fig. 17. Seismic profile (A - uninterpreted, B - interpreted) and variance attribute horizon slice (C - uninterpreted, D - interpreted) showing block falls with individual blocks reaching size of ~450 × 268 m (yellow arrow), related to steep slopes on the flanks of the thrust-cored anticlines. Location of seismic lines in Fig. 13. (For interpretation of the references to colour in this figure legend, the reader is referred to the Web version of this article.)

Zone are deposited close to the Atrato River delta (Fig. 2), with coarser particles only reaching the shelf break sporadically during the rainy season (Escobar and Velásquez-Montoya, 2018; Pujos and Javelaud, 1991). These sediment fluxes result in a muddy shelf edge that favours the development of mass failures. The failure scars created by these mass failures merge downslope and evolve into submarine canyons (Fig. 22). Similar configurations, where shelf-attached mass failures smooth topography created by tectonic deformation, are identified near the Baram river delta offshore northwest Borneo (Cullen, 2014; Morley and Leong, 2008).

5.4. Interaction of slope gradient, sediment supply and shelf width

We relate the three geomorphological zones in the southern Caribbean of Colombia with different combinations of sediment supply, slope gradient, and continental shelf width. We summarize these relationships in a ternary diagram (Fig. 23) that constitutes a predictive tool for the morphology and distribution of deep-water deposits in other compressional continental margins.

The Northern Zone, represented by the upper part of the ternary diagram, is characterized by high sediment supply, gentle slope topography, and narrow shelf width (Figs. 7 and 23). This zone exhibits large channel levee systems that cross the slope and continue for hundreds of kilometers through the bottom of the basin. In this zone, mass-transport deposits also occur, commonly associated with mass failures starting near the edge of the shelf where steeper gradients exist. The slope profiles associated with the channels and margin are 'mature' (Pettinga and Jobe, 2020), where high sediment supply is able to smooth out most tectonic deformation.

The Central Zone is represented by the left side of Fig. 23 and is characterized by a steep and irregular slope topography, low sediment supply and a moderate shelf width (Figs. 7 and 23). Here, the irregular relief created by tectonic deformation is the main control on sediment-dispersal patterns, and sediment supply cannot mature the slope profile (Cf. Pettinga and Jobe, 2020). This geomorphological zone is prone to mass wasting, with local mass failures from the crest of anticlines and to the development of submarine canyons cutting the anticlines.

Finally, the Southern Zone lies towards the lower right of Fig. 23, with high slope gradients, moderate to high sediment supply and a wide shelf (Figs. 7 and 23). In this zone, shelf-attached mass failures are the main mechanism for sediment transport. The erosional scours carved by mass flows merge downslope and evolve into submarine canyons that

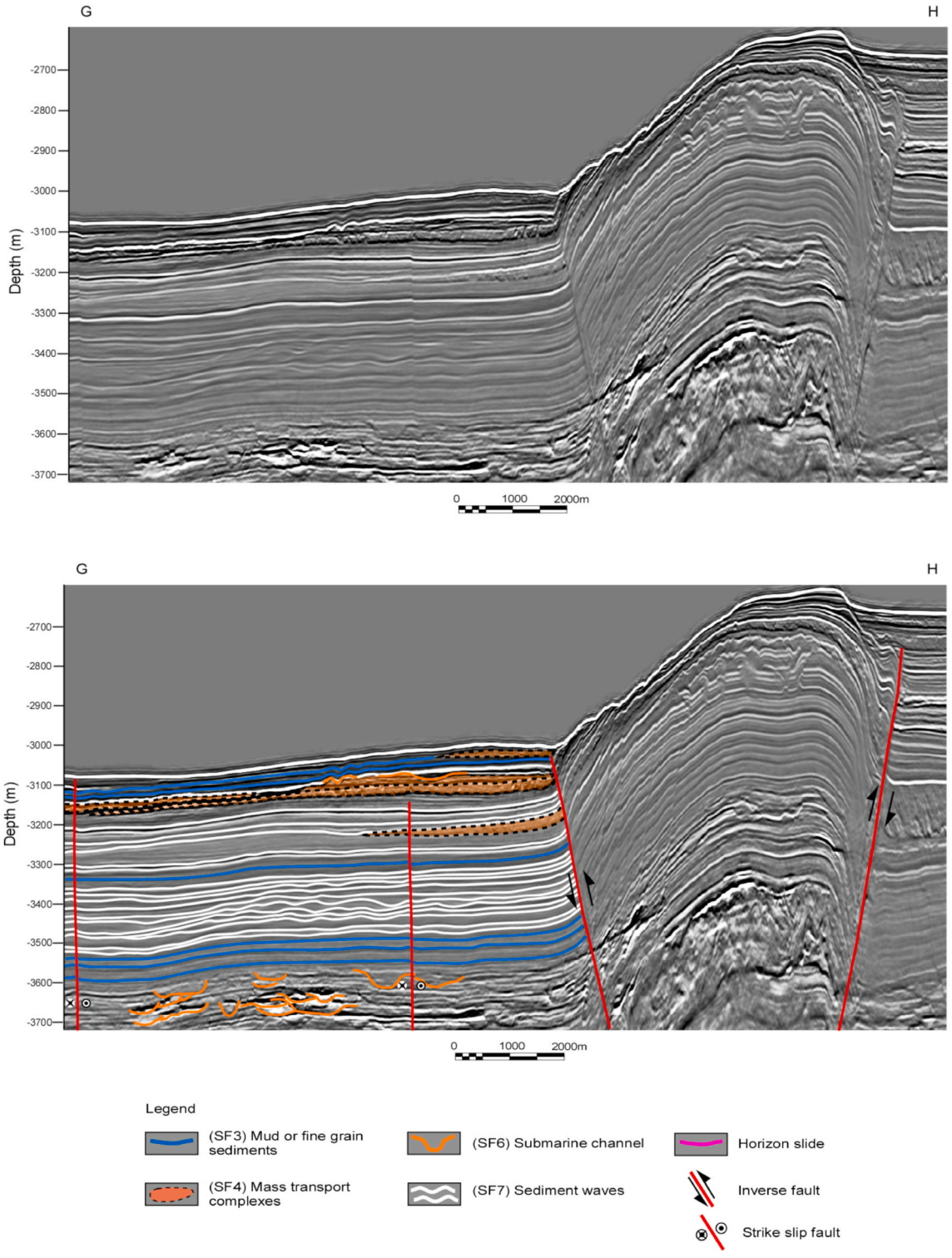

Fig. 18. Seismic profile (upper uninterpreted, lower interpreted) from Central Zone showing thrust-cored anticlines acting as topographic barriers to submarine canyon development, and creating areas at the bottom of the basin where sediment waves are preserved. See Fig. 13 for location.

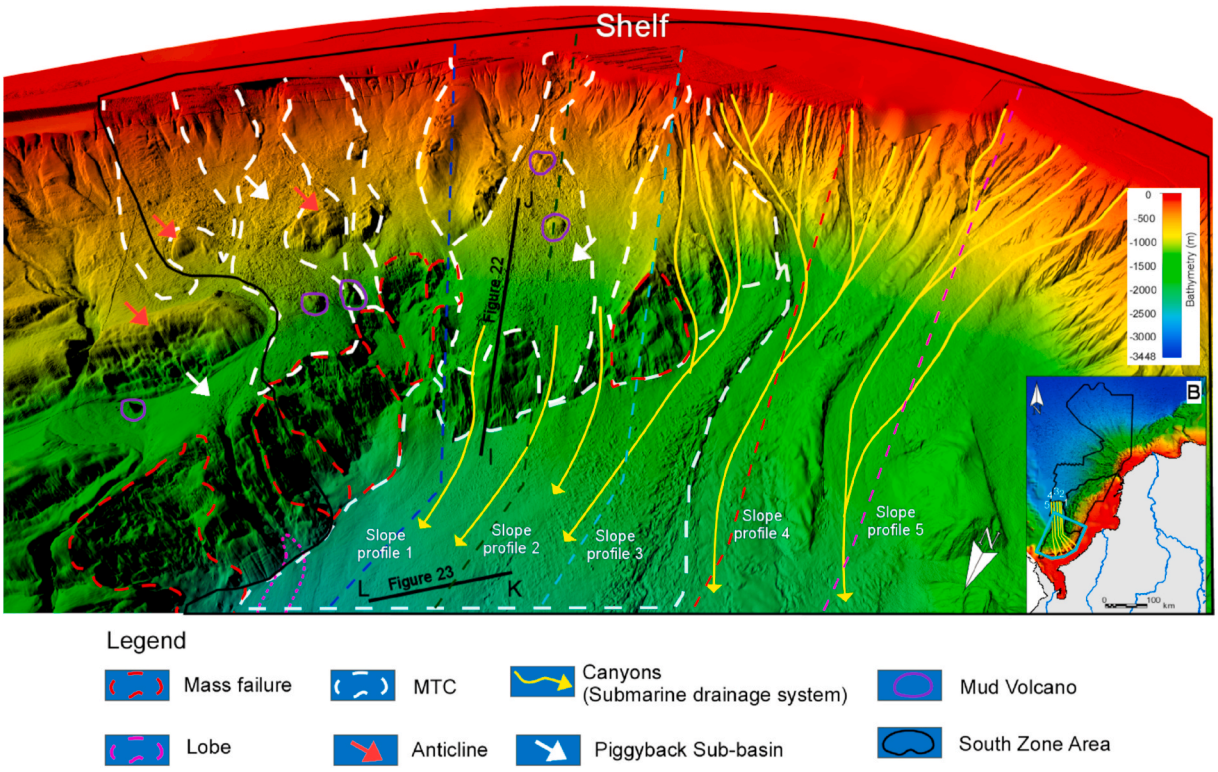

Fig. 19. 3D view of the bathymetry of the Southern Zone. Here the thrust belt has been greatly modified by mass wasting events that have eroded anticlinal crests and filled piggy-back sub-basins. Submarine canyons, which initiate in response to submarine failures, have developed over failure scars to become direct conduits for the transport of sediments from the slope to the distal basin, where sediments accumulate as unconfined mass transport complexes. The location of the image is indicated by the blue light box on the inset location map (B). Locations of slope profiles plotted in Fig. 21 and locations of Figs. 22 and 23. (For interpretation of the references to colour in this figure legend, the reader is referred to the Web version of this article.)

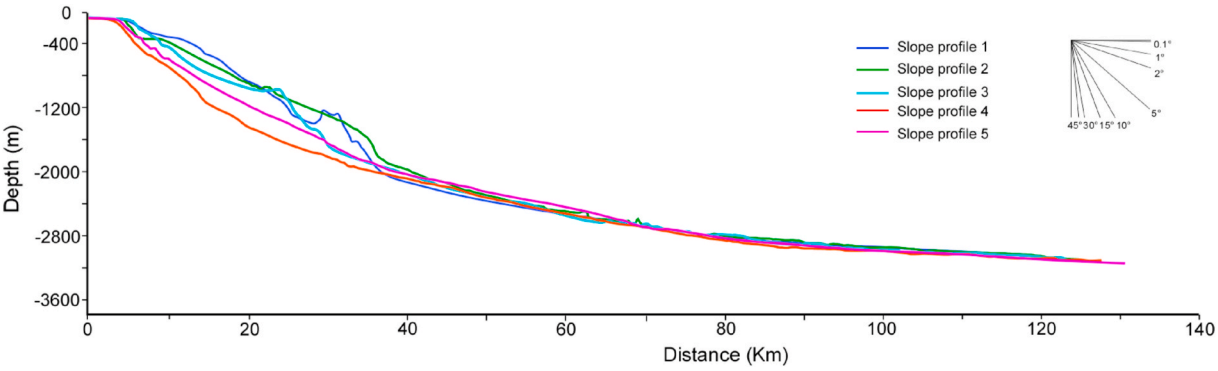

Fig. 20. Slope profiles through the Southern Zone with slopes ranging between ~2 and 5°. The steeper gradients are related with anticline crests that have not been degraded. Gentler slopes occur where mass-transport complexes have eroded anticlinal structures and filled piggyback sub-basins smoothing the topography. See Fig. 19 for location.

deliver mass-flows directly to the basin floor. This zone would be typified by a maturing or readjusting slope profile (Pettinga and Jobe, 2020).

This study shows that slope profile has a clear influence on morphology and character of deep-water deposits. The Southern Sinú Fold Belt creates an irregular slope in the Central and Southern Zones, where thrust-cored anticlines act as barriers for sediment transport from the continental shelf to the bottom of the basin, and piggy-back sub basins act as sediment sinks (Figs. 13–15). The rate at which the tectonic structures are degraded, and the slope profile is smoothed, is a function of sediment supply; these observations are corroborated by Pettinga and Jobe (2020), who link sediment supply to slope profile 'maturity' (i.e., roughness). In the Southern Zone, continuous mass-wasting driven by a high supply of fine-grained sediments has rapidly buried the fold belt, while in the Central Zone where sediment supply is lower, a more gradual degradation, driven by canyons that incise the anticlines and progressively connect piggy back sub-basins, has resulted in tortuous sediment-flow pathways (Vinnels et al., 2010) and irregular, immature slope topography. In the Northern Zone where tectonic deformation is less pronounced, and there is a high supply of mud-prone sediments, the system resembles mud-prone submarine fans in passive margins such as the Amazon Fan (Pirmez and Flood, 1995; Posamentier and Kolla, 2003; Romero-Otero et al., 2015).

The role of the shelf width on the architecture of deep-water deposits is less clear. In the Southern Zone where the shelf is widest, most of the sediments that reach the shelf-slope break are muddy, favoring the

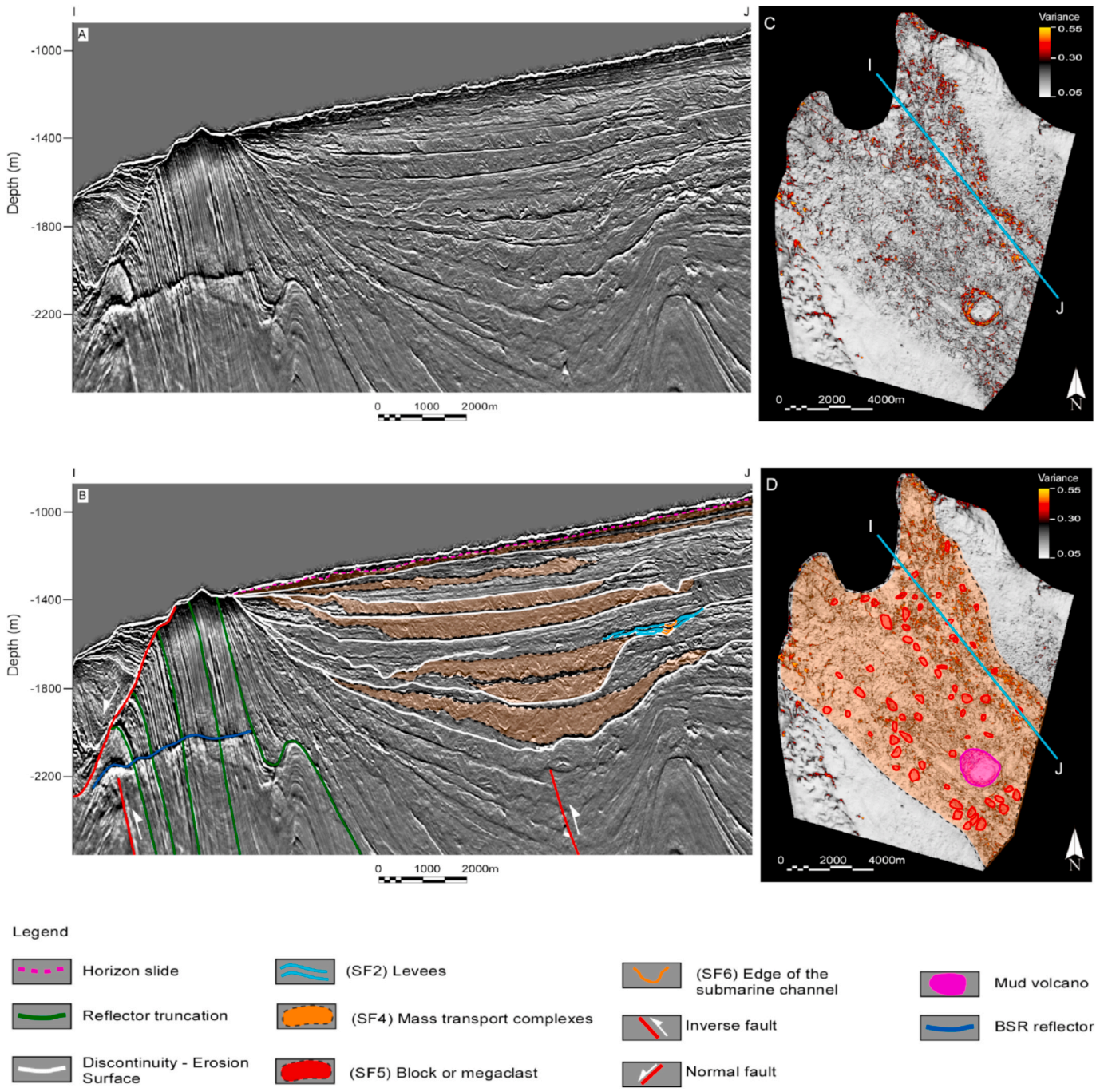

Fig. 21. Seismic profile (A - uninterpreted, B - interpreted) and variance attribute horizon slice (C - uninterpreted, D - interpreted) showing mass-transport complexes eroding and burying thrusted anticlines. The MTCs filled the intra-slope basins formed by synclines. Note the presence of megaclasts related with debris flows that originate in the upper slope and a mud volcano associated with the compressional deformation (horizon slice C, D). See Fig. 19 for location.

development of debris flows. We speculate that coarser (i.e., sandy) sediment is likely sequestered closer to the coastline, near the Atrato delta. However, in order to fully understand the impact of the shelf width on the sediment transfer from the river mouth to the slope, a more detailed characterization of the riverine sediment input at each of the river mouths, as well as a detailed study of the marine currents along the shelf would be required. Also, previous studies have demonstrated that the grain-size distribution of sediments influences the architecture of deep-water gravitational deposits (Jobe et al., 2015; Reading and Richards, 1994). Although we find linkages between sediment supply to each of the geomorphological zones and their resultant depositional architectures, the grain size distributions for each river are not available and hence the impact of grain-size on depositional architecture is not well understood.

6. Conclusions

We used high resolution bathymetric and 3D seismic data to analyze the complex interaction between shelf and slope morphology and sedimentation in a convergent margin with variable sediment supplies associated with different river systems.

- In convergent margins with deep-water thrust and fold belts such as the Colombian southern Caribbean, thrust-cored anticlines and

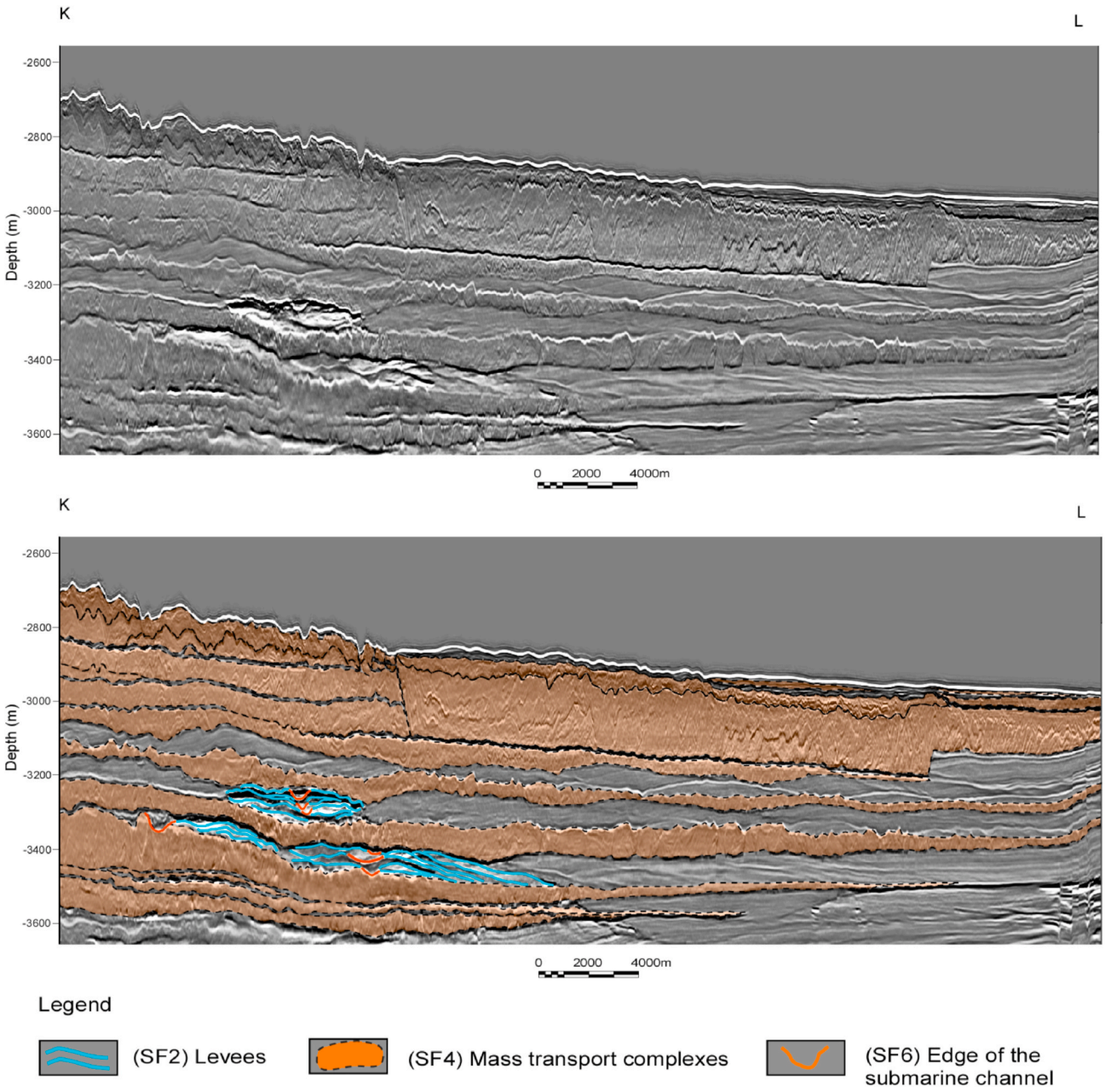

Fig. 22. Seismic line showing unconfined mass-transport complexes with amalgamated sizes up to 80 km long by 20 km wide and thicknesses exceeding 200 m, in the bottom of the basin, related to mass failures starting at shelf break in the Southern Zone. Note the presence of channel-levee systems fed by canyons that develop between mass failure events. See Fig. 19 for location.

piggyback sub-basins are the main barriers for sediment transport from the continental shelf to the basin floor.

- Tectonic relief is degraded and smoothed through erosion and sedimentation. The rate at which the tectonic structures are degraded, and the slope profile is smoothed, is a function of the steepness of the slope and sediment supply. Geomorphological zones with low sediment supply, high slope profiles and steep flanks related to anticlines, such as the Central Zone, are prone to mass wasting events that degrade anticlines and fill piggyback sub-basins. These mass flows commonly run out less than ~15 km. If areas with steep slopes receive high volumes of fine-grained sediments as in the Southern Zone, repeated mass failures attached to the shelf edge erode the tectonic structures, fill the piggyback sub-basins, and bury the fold belt. Moreover, if erosional scours carved by mass flows evolve into submarine canyons that confine mass flows, runout distances can surpass 80 km.
- Geomorphological zones where low slope gradients coexist with high supply of fine-grained sediments, like in the Northern Zone, are likely to display aggradational channel-levee systems that traverse the slope and continue onto the basin floor for hundreds of kilometers.

By comparing the spatial distribution and morphology of the depositional elements in areas with different shelf morphology and continental sediment inputs along the southern Colombian Caribbean margin, this study has enabled us to analyze the impact of three different factors controlling deep-water depositional patterns: slope profile, sediment input, and shelf width. These observations can be used as a tool to predict the depositional patterns more likely to develop in other

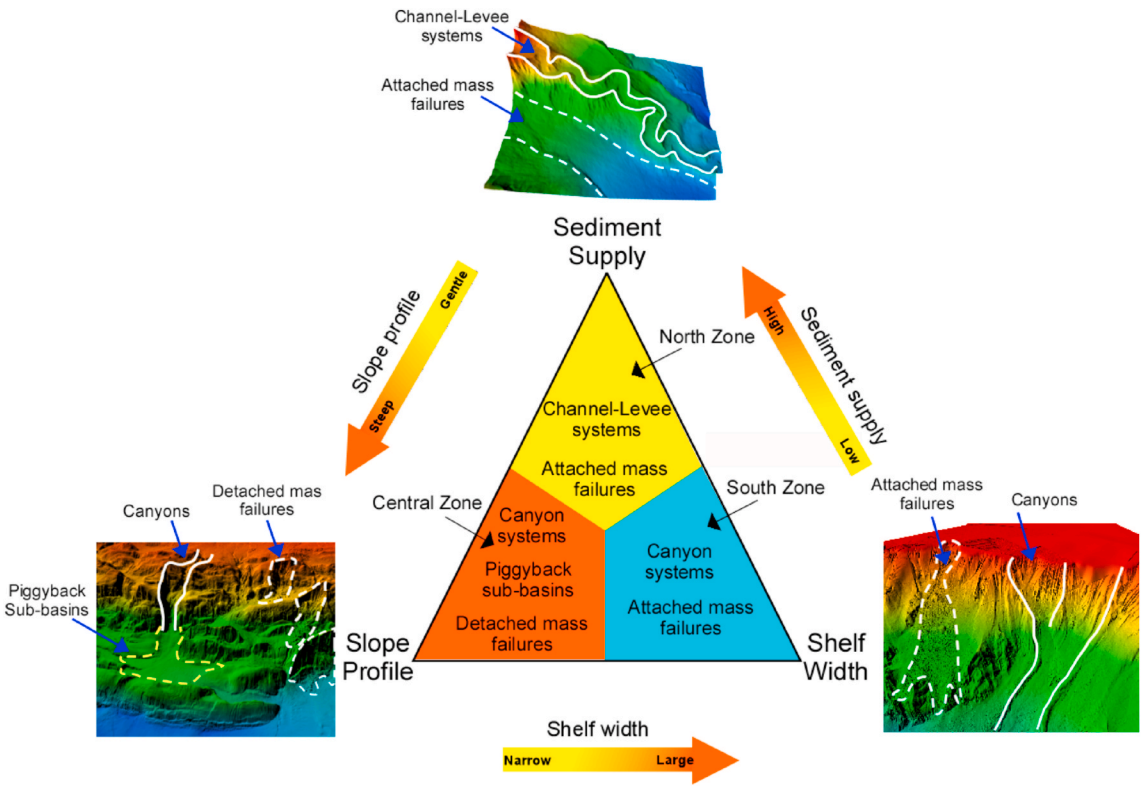

Fig. 23. Ternary diagram for deep-water deposit morphodynamics, showing geomorphological zones end-members associated with the complex interaction of sediment supply, slope profile, and continental shelf width in the southern Caribbean of Colombia convergent tectonic margin. (1) North Zone is characterized by high sediment supply (>100 × 106 Mg yr-1), gentle slope topography (<2°) and narrow shelf width (<50 km). (2) Central Zone have steep slope topography (>5°) low sediment supply (<10 × 106 Mg yr-1), and moderate shelf width (<50–100 km). (3) South Zone corresponds with steep slope topography (2–5°), high sediment supply (10–100 × 106 Mg yr-1) and large shelf width (>100 km). Modified from Prather (2003).

continental margins elsewhere, particularly those affected by deep-water fold belts.

CRediT authorship contribution statement

J. Naranjo-Vesga: Conceptualization, Methodology, Writing - original draft. **A. Ortiz-Karpf:** Supervision, Conceptualization, Methodology, Writing - review & editing. **L. Wood:** Supervision, Conceptualization, Methodology, Writing - review & editing. **Z. Jobe:** Supervision, Conceptualization, Methodology, Writing - review & editing, Software. **J.F. Paniagua-Arroyave:** Supervision, Conceptualization, Methodology, Writing - review & editing. **L. Shumaker:** Conceptualization, Methodology, Software. **D. Mateus-Tarazona:** Conceptualization. **P. Galindo:** Conceptualization.

Declaration of competing interest

The authors declare that they have no known competing financial interests or personal relationships that could have appeared to influence the work reported in this paper.

Acknowledgments

These results are a contribution of the study *Adaptación de metodologías para evaluación de geohazards y seahazards en el Caribe Colombiano*, developed at Instituto Colombiano del Petróleo. Ecopetrol S.A provided funding, bathymetry, and seismic data. The authors also thank EAFIT University and MinCiencias of Colombia (Colciencias) with the public call 758 of 2016, for the funds and all support provided to achieve these results. Many thanks to an anonymous reviewer who provided valuable comments that improved the quality of this article.

Appendix A. Supplementary data

Supplementary data to this article can be found online at https://doi.org/10.1016/j.marpetgeo.2020.104639.

References

Abreu, V., Sullivan, M., Pirmez, C., Mohrig, D., 2003. Lateral accretion packages (LAPs): an important reservoir element in deep water sinuous channels. Mar. Petrol. Geol. 20, 631–648. https://doi.org/10.1016/j.marpetgeo.2003.08.003.

Alfaro, E., Holz, M., 2014. Seismic geomorphological analysis of deepwater gravity-driven deposits on a slope system of the southern Colombian Caribbean margin. Mar. Petrol. Geol. 57, 294–311. https://doi.org/10.1016/j.marpetgeo.2014.06.002.

Armitage, D.A., McHargue, T., Fildani, A., Graham, S.A., 2012. Postavulsion channel evolution: Niger Delta continental slope. Am. Assoc. Petrol. Geol. Bull. 96, 823–843. https://doi.org/10.1306/09131110189.

Barat, F., Mercier de Lépinay, B., Sosson, M., Müller, C., Baumgartner, P.O., Baumgartner-Mora, C., 2014. Transition from the farallon plate subduction to the collision between south and Central America: geological evolution of the Panama isthmus. Tectonophysics 622, 145–167. https://doi.org/10.1016/j.tecto.2014.03.008.

Bernal-Olaya, R., Sanchez, J., Mann, P., Murphy, M., 2015. Along-strike crustal thickness variations of the subducting Caribbean plate produces two distinctive styles of thrusting in the offshore South Caribbean deformed belt, Colombia. Mem. 108 Pet. Geol. Potential Colomb. Caribb. Margin 295–322. https://doi.org/10.1306/13531941m1083645.

Bourget, J., Zaragosi, S., Ellouz-Zimmermann, N., Mouchot, N., Garlan, T., Schneider, J. L., Lanfumey, V., Lallemant, S., 2011. Turbidite system architecture and sedimentary processes along topographically complex slopes: the Makran convergent margin. Sedimentology 58, 376–406. https://doi.org/10.1111/j.1365-3091.2010.01168.x.

Cadena, A.F., Romero, G., Slatt, R., 2015. Application of stratigraphic grade concepts to understand basin-fill processes and deposits in an active margin setting, Magdalena submarine fan and associated fold-and-thrust belts, offshore Colombia. In: Memoir 108: Petroleum Geology and Potential of the Colombian Caribbean Margin. AAPG, pp. 323–344. https://doi.org/10.1306/13531942M1083646.

Catuneanu, O., 2020. Sequence stratigraphy of deep-water systems. Mar. Petrol. Geol. 114, 104238. https://doi.org/10.1016/j.marpetgeo.2020.104238.

Catuneanu, O., 2002. Sequence stratigraphy of clastic systems. J. Afr. Earth Sci. 35, 1–43.

Cediel, F., Shaw, R.P., Cáceres, C., 2005. Tectonic assembly of the northern andean block. AAPG Mem 815–848.
Chima, K.I., Do Couto, D., Leroux, E., Gardin, S., Hoggmascall, N., Rabineau, M., Granjeon, D., Gorini, C., 2019. Seismic stratigraphy and depositional architecture of Neogene intraslope basins, offshore western Niger Delta. Mar. Petrol. Geol. 109, 449–468. https://doi.org/10.1016/j.marpetgeo.2019.06.030.
Clark, I.R., Cartwright, J.A., 2009. Interactions between submarine channel systems and deformation in deepwater fold belts: examples from the Levant Basin, Eastern Mediterranean sea. Mar. Petrol. Geol. 26, 1465–1482. https://doi.org/10.1016/j.marpetgeo.2009.05.004.
Correa-Ramirez, M., Rodriguez-Santana, Á., Ricaurte-Villota, C., Paramo, J., 2020. The Southern Caribbean upwelling system off Colombia: water masses and mixing processes. Deep. Res. Part I Oceanogr. Res. Pap. 155 https://doi.org/10.1016/j.dsr.2019.103145.
Corredor, F., 2003. Seismic strain rates and distributed continental deformation in the northern Andes and three-dimensional seismotectonics of northwestern South America. Tectonophysics 372, 147–166. https://doi.org/10.1016/S0040-1951(03)00276-2.
Cortés, M., Angelier, J., 2005. Current states of stress in the northern Andes as indicated by focal mechanisms of earthquakes. Tectonophysics 403, 29–58. https://doi.org/10.1016/j.tecto.2005.03.020.
Cullen, A., 2014. Nature and significance of the west Baram and tinjar lines, NW Borneo. Mar. Petrol. Geol. 51, 197–209. https://doi.org/10.1016/j.marpetgeo.2013.11.010.
Deptuck, M.E., Steffens, G.S., Barton, M., Pirmez, C., 2003. Architecture and evolution of upper fan channel-belts on the Niger Delta slope and in the Arabian Sea. Mar. Petrol. Geol. 20, 649–676. https://doi.org/10.1016/j.marpetgeo.2003.01.004.
Deptuck, M.E., Sylvester, Z., O'byrne, C., 2012. Pleistocene seascape evolution above a "simple" stepped slope—western Niger delta. Appl. Princ. Seism. Geomorphol. to Cont. Base-of-Slope Syst. Case Stud. from Seafloor Near-Seafloor Analog 199–222. https://doi.org/10.2110/pec.12.99.0199.
Dorschel, B., Wheeler, A.J., Monteys, X., Verbruggen, K., 2010. Atlas of the Deep-Water Seabed, Dk. Springer Netherlands, Dordrecht. https://doi.org/10.1007/978-90-481-9376-9.
Duque-Caro, H., 1990. The choco block in the northwestern corner of South America: structural, tectonostratigraphic, and paleogeographic implications. J. South Am. Earth Sci. 3, 71–84. https://doi.org/10.1016/0895-9811(90)90019-W.
Duque-Caro, H., 1979. Major structural elements and evolution of northwestern Colombia. AAPG Mem. 29 Geol. Geophys. Investig. Cont. Margins 329–351.
Ercilla, G., Alonso, B., Estrada, F., Chiocci, F.L., Baraza, J., Farran, M.L., 2002a. The Magdalena turbidite system (caribbean sea): present-day morphology and architecture model. Mar. Geol. 185, 303–318. https://doi.org/10.1016/S0025-3227(02)00182-2.
Ercilla, G., Wynn, R.B., Alonso, B., Baraza, J., 2002b. Initiation and evolution of turbidity current sediment waves in the Magdalena turbidite system. Mar. Geol. 192, 153–169. https://doi.org/10.1016/S0025-3227(02)00553-4.
Escalona, A., Mann, P., 2011. Tectonics , basin subsidence mechanisms , and paleogeography of the Caribbean-South American plate boundary zone. JMPG 28, 8–39. https://doi.org/10.1016/j.marpetgeo.2010.01.016.
Escobar, C.A., Velásquez-Montoya, L., 2018. Modeling the sediment dynamics in the gulf of Urabá colombian Caribbean sea. Ocean. Eng. 147, 476–487. https://doi.org/10.1016/j.oceaneng.2017.10.055.
Escobar, C.A., Velásquez, L., Posada, F., 2015. Marine currents in the gulf of Urabá, Colombian caribbean sea. J. Coast Res. 316, 1363–1374. https://doi.org/10.2112/jcoastres-d-14-00186.1.
Estrada, F., Ercilla, G., Alonso, B., 2005. Quantitative study of a Magdalena submarine channel (Caribbean Sea): implications for sedimentary dynamics. Mar. Petrol. Geol. 22, 623–635. https://doi.org/10.1016/j.marpetgeo.2005.01.004.
Faugères, J.-C, Mulder, T, 2011. Contour currents and contourite drifts. Dev. Sedimentol. 63, 149–214. https://doi.org/10.1016/B978-0-444-53000-4.00003-2.
Flinch, J., Amaral, J., Doulcet, A., Mouly, B., Osorio, C., Pince, J.M., 2003. Structure of the offshore sinu accretionary wedge . Northern Colombia. VIII simp. Boliv. Cuencas Subandinas 76–83.
Galindo, P., Lonergan, L., 2020. Basin evolution and shale tectonics on an obliquely convergent margin: the bahia basin, offshore Colombian caribbean. Tectonics 39. https://doi.org/10.1029/2019tc005787.
Gamboa, D., Alves, T., Cartwright, J., 2011. Distribution and characterization of failed (mega)blocks along salt ridges, southeast Brazil: implications for vertical fluid flow on continental margins. J. Geophys. Res. Solid Earth 116, 1–20. https://doi.org/10.1029/2011JB008357.
Idárraga-García, J., Masson, D.G., García, J., León, H., Vargas, C.A., 2019. Architecture and development of the Magdalena submarine fan (southwestern caribbean). Mar. Geol. 414, 18–33. https://doi.org/10.1016/j.margeo.2019.05.005.
Idárraga-García, J., Vargas, C.A., 2014. Morphological expression of submarine landslides in the accretionary prism of the caribbean continental margin of Colombia. In: Krastel, S., Behrmann, J.-H., Völker, D., Stipp, M., Berndt, C., Urgeles, R., Chaytor, J., Huhn, K., Strasser, M., Bonnevie Harbitz, C. (Eds.), Submarine Mass Movements and Their Consequences: Advances in Natural and Technological Hazards Research. Springer, pp. 391–401. https://doi.org/10.1007/978-3-319-00972-8_35.
Jackson, C.A.L., 2011. Three-dimensional seismic analysis of megaclast deformation within a mass transport deposit; Implications for debris flow kinematics. Geology 39, 203–206. https://doi.org/10.1130/G31767.1.
Jervey, M.T., 1988. Quantitative Geological Modeling of Siliciclastic Rock Sequences and Their Seismic Expression. SEPM Spec. Publ. https://doi.org/10.2110/pec.88.01.0047.
Jobe, Z.R., Howes, N.C., Auchter, N.C., 2016. Comparing submarine and fluvial channel kinematics: implications for stratigraphic architecture. Geology 44, 931–934. https://doi.org/10.1130/G38158.1.
Jobe, Z.R., Lowe, D.R., Uchytil, S.J., 2011. Two fundamentally different types of submarine canyons along the continental margin of Equatorial Guinea. Mar. Petrol. Geol. 28, 843–860. https://doi.org/10.1016/j.marpetgeo.2010.07.012.
Jobe, Z.R., Sylvester, Z., Parker, A.O., Howes, N., Slowey, N., Pirmez, C., 2015. Rapid adjustment of submarine channel architecture to changes in sediment supply. J. Sediment. Res. 85, 729–753. https://doi.org/10.2110/jsr.2015.30.
Jolly, B.A., Anyiam, O.A., Omeru, T., 2017. Structural controls on channel-related seismic facies distribution in the toe-thrust of deepwater Niger Delta. J. Afr. Earth Sci. 125, 151–165. https://doi.org/10.1016/j.jafrearsci.2016.11.012.
Kolla, V., Buffler, R.T., 1985. Magdalena fan, caribbean. In: Bouma, A.H., Normark, W.R. (Eds.), Submarine Fans and Related Turbidite Systems. Frontiers in Sedimentary Geology. Springer, New York, NY. https://doi-org.ezproxy.eafit.edu.co/10.1007/978-1-4612-5114-9_12.
Kolla, V., Buffler, R.T., 1984a. Morphologic, acoustic, and sedimentologic characteristics of the Magdalena Fan. Geo Mar. Lett. 3, 85–91. https://doi.org/10.1007/BF02462452.
Kolla, V., Buffler, R.T., 1984b. Seismic stratigraphy and sedimentation of Magdalena fan, southern Colombian basin, caribbean sea. Am. Assoc. Petrol. Geol. Bull. 68, 316–332. https://doi.org/10.1306/ad460a1c-16f7-11d7-8645000102c1865d.
Ma, H.X., Fan, G.Z., Shao, D.L., Ding, L.B., Sun, H., Zhang, Y., Zhang, Y.G., Cronin, B.T., 2020. Deep-water depositional architecture and sedimentary evolution in the Rakhine Basin, northeast Bay of Bengal. Petrol. Sci. 17, 598–614. https://doi.org/10.1007/s12182-020-00442-0.
Martinez, J.A., Castillo, J., Ortiz-Karpf, A., Rendon, L., Mosquera, J.C., Vega, V., 2015. Deep water untested oil-play in the Magdalena fan, caribbean Colombian basin. In: Bartolini, C., Mann, P. (Eds.), Petroleum Geology and Potential of the Colombian Caribbean Margin, vol. 108. American Association of Petroleum Geologists, Memoir, pp. 251–260. https://doi.org/10.1306/13531955m1083658.
Mayall, M., Lonergan, L., Bowman, A., James, S., Mills, K., Primmer, T., Pope, D., Rogers, L., Skeene, R., 2010. The response of turbidite slope channels to growth-induced seabed topography. Am. Assoc. Petrol. Geol. Bull. 94, 1011–1030. https://doi.org/10.1306/01051009117.
McAdoo, B.G., Pratson, L.F., Orange, D.L., 2000. Submarine landslide geomorphology, US continental slope. Mar. Geol. https://doi.org/10.1016/S0025-3227(00)00050-5.
Milliman, J.D., Meade, R.H., 1983. World-wide delivery of river sediment to the oceans. J. Geol. 91 https://doi.org/10.1086/628741.
Moreno-Madriñán, M.J., Rickman, D.L., Ogashawara, I., Irwin, D.E., Ye, J., Al-Hamdan, M.Z., 2015. Using remote sensing to monitor the influence of river discharge on watershed outlets and adjacent coral Reefs: Magdalena River and Rosario Islands, Colombia. Int. J. Appl. Earth Obs. Geoinf. 38, 204–215. https://doi.org/10.1016/j.jag.2015.01.008.
Morley, C.K., King, R., Hillis, R., Tingay, M., Backe, G., 2011. Deepwater fold and thrust belt classification, tectonics, structure and hydrocarbon prospectivity: a review. Earth Sci. Rev. 104, 41–91. https://doi.org/10.1016/j.earscirev.2010.09.010.
Morley, C.K., Leong, L.C., 2008. Evolution of deep-water synkinematic sedimentation in a piggyback basin, determined from three-dimensional seismic reflection data. Geosphere 4, 939–962. https://doi.org/10.1130/GES00148.1.
Moscardelli, L., Wood, L., 2008. New classification system for mass transport complexes in offshore Trinidad. Basin Res. 20, 73–98. https://doi.org/10.1111/j.1365-2117.2007.00340.x.
Moscardelli, L., Wood, L., Mann, P., 2006. Mass-transport complexes and associated processes in the offshore area of Trinidad and Venezuela. Am. Assoc. Petrol. Geol. Bull. 90, 1059–1088. https://doi.org/10.1306/02210605052.
Mutti, E., 1985. Provenance of arenites. In: Zuffa, G.G. (Ed.), Provenance of Arenites. Reidel Publishing Company, Dordrecht, pp. 65–93. https://doi.org/10.1007/978-94-017-2809-6.
Oluboyo, A.P., Gawthorpe, R.L., Bakke, K., Hadler-Jacobsen, F., 2014. Salt tectonic controls on deep-water turbidite depositional systems: miocene, southwestern Lower Congo Basin, offshore Angola. Basin Res. 26, 597–620. https://doi.org/10.1111/bre.12051.
Ortiz-Karpf, A., Hodgson, D.M., Jackson, C.A.-L., McCaffrey, W.D., 2017. Influence of seabed morphology and substrate composition on mass-transport flow processes and pathways: insights from the Magdalena fan, offshore Colombia. J. Sediment. Res. 87, 189–209. https://doi.org/10.2110/jsr.2017.10.
Ortiz-Karpf, A., Hodgson, D.M., Jackson, C.A.L., McCaffrey, W.D., 2016. Mass-transport complexes as markers of deep-water fold-and-thrust belt evolution: insights from the southern Magdalena fan, offshore Colombia. Basin Res. 30, 65–88. https://doi.org/10.1111/bre.12208.
Ortiz-Karpf, A., Hodgson, D.M., McCaffrey, W.D., 2015. The role of mass-transport complexes in controlling channel avulsion and the subsequent sediment dispersal patterns on an active margin: the Magdalena Fan, offshore Colombia. Mar. Petrol. Geol. 64, 58–75. https://doi.org/10.1016/j.marpetgeo.2015.01.005.
Pettinga, L., Jobe, Z., Shumaker, L., Howes, N., 2018. Morphometric scaling relationships in submarine channel-lobe systems. Geology 46, 819–822. https://doi.org/10.1130/G45142.1.
Pettinga, L.A., Jobe, Z.R., 2020. How submarine channels (re)shape continental margins. J. Sediment. Res.
Piper, D.J.W., Deptuck, M.E., Mosher, D.C., Hughes Clarke, J.E., Migeon, S., 2012. Erosional and depositional features of glacial meltwater discharges on the eastern Canadian continental margin. Appl. Princ. Seism. Geomorphol. to Cont. Base-of-Slope Syst. Case Stud. from Seafloor Near-Seafloor Analog 61–80. https://doi.org/10.2110/pec.12.99.0061.

Pirmez, C., Beaubouef, R., Friedmann, S., Mohrig, D., 2000. Equilibrium profile and baselevel in submarine channels: examples from late pleistocene systems and implications for the architecture of deepwater reservoirs. In: Paul, Weimer (Ed.), Deep-Water Reservoirs of the World: Gulf Coast Section SEPM Foundation, 20th Annual Research Conference. SEPM (Society for Sedimentary Geology), Houston, pp. 782–805 https://doi.org/10.5724/gcs.00.20.

Pirmez, C., Flood, R.D., 1995. Morphology and structure of Amazon channel. Proc. Ocean Drill. Program 155. https://doi.org/10.2973/odp.proc.ir.155.103.1995. Initial Reports 155.

Posamentier, H.W., Kolla, V., 2003. Seismic geomorphology and stratigraphy of depositional elements in deep-water settings. J. Sediment. Res. 73, 367–388. https://doi.org/10.1306/111302730367.

Posamentier, H.W., Meizarwin, Wisman, P.S., Plawman, T., 2000. Deep water depositional systems—ultra-deep makassar strait, Indonesia. In: Weimer, P., Slatt, R. M., Coleman, J., Rosen, N.C., Nelson, H., Bouma, A.H., Styzen, M.J., Lawrence, D.T. (Eds.), Deep-Water Reservoirs of the World: Gulf Coast Section SEPM Foundation, 20th Annual Research Conference, pp. 806–816. https://doi.org/10.5724/gcs.00.15.0806.

Posamentier, H.W., Walker, R.G., 2006. Facies Models Revisited, Special Pu. SEPM (Society for Sedimentary Geology), Oklahoma.

Prather, B.E., 2003. Controls on reservoir distribution, architecture and stratigraphic trapping in slope settings. Mar. Petrol. Geol. 20, 529–545. https://doi.org/10.1016/j.marpetgeo.2003.03.009.

Prather, B.E., 2000. Calibration and visualization of depositional process models for above-grade slopes: a case study from the Gulf of Mexico. Mar. Petrol. Geol. 17, 619–638. https://doi.org/10.1016/S0264-8172(00)00015-5.

Prather, B.E., Booth, J.R., Steffens, G.S., Craig, P.A., 1998. Classification, lithologic calibration, and stratigraphic succession of seismic facies of intraslope basins, deep-water Gulf of Mexico. Am. Assoc. Petrol. Geol. Bull. 82, 701–728. https://doi.org/10.1306/1d9bc5d9-172d-11d7-8645000102c1865d.

Pujos, M., Javelaud, O., 1991. Depositional facies of a mud shelf between the Sinú river and the Darien Gulf (Caribbean coast of Colombia): environmental factors control its sedimentation and origin of deposits. Continent. Shelf Res. 11, 601–623.

Rangel-Buitrago, N., Idárraga-García, J., 2010. Geología general, morfología submarina y facies sedimentarias en el margen continental y los fondos oceánicos del mar caribe colombiano. In: Biodiversidad Del Margen Continental Del Caribe Colombiano, p. 457.

Reading, H.G., Richards, M., 1994. Turbidite systems in deep-water basin margins classified by grain size and feeder system. Am. Assoc. Petrol. Geol. Bull. 78, 792–822. https://doi.org/10.1306/A25FE3BF-171B-11D7-8645000102C1865D.

Restrepo, J.D., Kjerfve, B., 2004. The pacific and caribbean rivers of Colombia: water discharge, sediment transport and dissolved loads. In: Drude de Lacerda, L., Santelli, R.E., Duursma, E.K., Abrao, J.J. (Eds.), Environmental Geochemistry in Tropical and Subtropical Environments. Springe-Verlag Berlin Heidelberg. https://doi.org/10.1007/978-3-662-07060-4.

Romero-Otero, G.A., 2009. Deepwater Sedimentary Processes in an Active Margin, Magdalena Submarine Fan, Offshore Colombia. The University of Oklahoma.

Romero-Otero, G.A., Slatt, R.M., Pirmez, C., 2015. Evolution of the Magdalena deepwater fan in a tectonically active setting, offshore Colombia. AAPG Mem 108, 675–707. https://doi.org/10.1306/13531953m1083656.

Ruiz, C., Davis, N., Bentham, P., Price, A., Carvajal, D., 2000. Structure and tectonic evolution of the south caribbean basin, southern offshore Colombia: a progressive accretionary prism. In: VII Simp. Boliv. - Explor. Pet. en las Cuencas Subandinas, vol. 22.

Shanmugam, G., 2016. Slides, Slumps, Debris Flows, Turbidity Currents, and Bottom Currents. Elsevier.

Shumaker, L.E., Jobe, Z.R., Johnstone, S.A., Pettinga, L.A., Cai, D., Moody, J.D., 2018. Controls on submarine channel-modifying processes identified through morphometric scaling relationships. Geosphere 14, 2171–2187. https://doi.org/10.1130/GES01674.1.

Sinclair, H.D., Tomasso, M., 2007. Depositional evolution of confined turbidite basins. J. Sediment. Res. 72, 451–456. https://doi.org/10.1306/111501720451.

Smith, R., 2004. Silled sub-basins to connected tortuous corridors: sediment distribution systems on topographically complex sub-aqueous slopes. Geol. Soc. Spec. Publ. 222, 23–43. https://doi.org/10.1144/GSL.SP.2004.222.01.03.

Sømme, T.O., Jackson, C.A.L., 2013. Source-to-sink analysis of ancient sedimentary systems using a subsurface case study from the Møre-Trøndelag area of southern Norway: Part 2 - sediment dispersal and forcing mechanisms. Basin Res. 25, 512–531. https://doi.org/10.1111/bre.12014.

Spikings, R., Cochrane, R., Villagomez, D., Van der Lelij, R., Vallejo, C., Winkler, W., Beate, B., 2015. The geological history of northwestern South America: from pangaea to the early collision of the caribbean large igneous province (290-75 ma). Gondwana Res. 27, 95–139. https://doi.org/10.1016/j.gr.2014.06.004.

Stow, D.A.V., Piper, D.J.W., 1984. Deep-water fine-grained sediments; history, methodology and terminology. Geol. Soc. London, Spec. Publ. 15, 3–14. https://doi.org/10.1144/GSL.SP.1984.015.01.01.

Sweet, M.L., Blum, M.D., 2016. Connections between fluvial to shallow marine environments and submarine canyons: implications for sediment transfer to deep water. J. Sediment. Res. 86, 1147–1162. https://doi.org/10.2110/jsr.2016.64.

Sylvester, Z., Deptuck, M.E., Prather, B.E., Pirmez, C., O'byrne, C., 2012. Seismic Stratigraphy of a Shelf-Edge Delta and Linked Submarine Channels in the Northeastern Gulf of Mexico, Application of the Principles of Seismic Geomorphology to Continental-Slope and Base-Of-Slope Systems: Case Studies from Seafloor and Near-Seafloor Analogues. https://doi.org/10.2110/pec.12.99.0031.

Symithe, S., Calais, E., Chabalier, J.B. De, Robertson, R., Higgins, M., 2015. Journal of geophysical research: solid earth current block motions and strain accumulation on active faults in the caribbean. J. Geophys. Res. Solid Earth 3748–3774. https://doi.org/10.1002/2014JB011779 (Received).

Taboada, A., Rivera, L.A., Fuenzalida, A., Cisternas, A., Philip, H., Bijwaard, H., Olaya, J., Rivera, C., 2000. Geodynamics of the northern Andes: subductions and intracontinental deformation (Colombia). Tectonics 19, 787–813. https://doi.org/10.1029/2000TC900004.

Vinnels, J.S., Butler, R.W.H., McCaffrey, W.D., Paton, D.A., 2010. Depositional processes across the Sinú accretionary prism, offshore Colombia. Mar. Petrol. Geol. 27, 794–809. https://doi.org/10.1016/j.marpetgeo.2009.12.008.